PHOTOTHERMAL ABLATION OF LIVER TISSUE WITH 1940-NM THULIUM FIBER LASER: ABLATION EFFICIENCY AND TEMPERATURE MEASUREMENTS

by

Heba Alagha

B.S., Computer Engineering, University Of Jordan, 2005

Submitted to the Institute of Biomedical Engineering
in partial fulfillment of the requirements
for the degree of
Master of Science
in
Biomedical Engineering

Boğaziçi University
2015

ACKNOWLEDGMENTS

First and foremost, it gives me a great pleasure to express my deepest gratitude and respect to my thesis supervisor Prof. Dr. Murat Gülsoy for his patient and constant guidance throughout my thesis. Without his moral support, encouragement, motivation, and invaluable advice, this thesis would not have been possible. I have been extremely lucky to have a supervisor who cared so much about my work, and who responded to my questions and queries so promptly and gently. I simply cannot think of a better supervisor.

Besides, I would like to thank the members of my thesis committee Prof. Dr. Inci Çilesiz and Asst. Prof. Dr. Bora Garipcan for spending their time on careful reading of my thesis as well as for their valuable comments.

I would also like to acknowledge Burc Tunç for her invaluable help and suggestions during my experiments, Özgür Kaya for his help throughout my thesis work, Ayşe Sena Sarp and Nermin Topaloğlu for their friendly support and care, and all my colleagues in the Biophotonics laboratory for their support.

Words fail me to express my love and appreciation to my late mother Dr. Ferial for everything she did for me and for being my hero and role model in every aspect of life, and to my father Dr. Zakaria for his endless love and support and for being always there for me. Everything I am today I owe to them.

Last but not least, I would like to express my huge warm thanks to my lovely husband Raif for his sincere support and encouragement, to my Mohammed and Noha for being the joy of my life, and to my whole family for their support.

To the memory of my beloved mother

ABSTRACT

PHOTOTHERMAL ABLATION OF LIVER TISSUE WITH 1940-NM THULIUM FIBER LASER: ABLATION EFFICIENCY AND TEMPERATURE MEASUREMENTS

The purpose of this study was to investigate the effectiveness of 1940-nm Thulium fiber laser for liver surgery. This was done by determining the ablation efficiency of different working modes and power settings of 1940-nm Thulium fiber laser on liver tissue, in addition to utilizing a real time temperature monitoring to provide the necessary feedback for adjusting laser parameters to minimize the collateral thermal damage to adjacent tissues.

Thulium fiber laser was delivered to lamb liver tissue samples via 400 μm flat-cut bare-ended tip fiber in contact mode. Continuous-wave and pulsed modes were used, each at 4 different laser power values (200, 400, 600, and 800 mW) and exposure times. Exposure times were chosen to give the same total applied energy of 4J for comparison purposes. A total of 64 laser applications were performed in order to study 8 laser parameter combinations with each parameter combination repeated 8 times. Following laser irradiation, tissues were processed and stained with H&E for macroscopic evaluation of ablation and total altered areas, and ablation efficiencies were calculated. Temperature of the nearby tissue was measured using a K-type thermocouple that was inserted at a distance of 1 mm from the fiber, and rate of temperature change was calculated.

A strong correlation between the rate of temperature change and ablation area was depicted. Larger ablation and total altered areas were obtained for higher power values for both continuous-wave and pulsed modes, while ablation efficiencies were not significantly different. Continuous mode yielded higher ablation and total altered areas, and higher ablations efficiencies than pulsed mode. Histological evaluation revealed a narrow vacuolization zone and negligible carbonization for higher power values.

Keywords: Laser Surgery, Liver Surgery, Thulium Fiber Laser, 1940-nm.

ÖZET

1940-NM TULYUM FİBER LASERİN KARACIĞER DOKU FOTOTERMAL ABLASYON: ABLASYON VERİMLİLİĞİ VE SICAKLIK ÖLÇÜMLERİ

Bu çalışmanın amacı 1940-nm Tulyum fiber laserin karaciğer cerrahisinde etkinliğini araştırmaktır. Bu amaçla çeşitli çalışma yöntemleriyle ve farklı güçlerde uygulanan 1940-nm Tulyum fiber laserin karaciğer dokusu üzerindeki ablasyon etkinliği belirlendi. Laser uygulamaları esnasında gerçek zamanlı sıcaklık ölçümü geri besleme tekniği ile laser parametrelerini düzenlemek için kullanıldı ve çevre dokularda oluşan ısıl hasar en aza indirgendi.

Bu çalışmada taze kuzu karaciğer dokuları kullanıldı. Laser ışıması, 400 μm merkez çapa sahip olan çıplak uçlu optik lifler ile doku örneklerine temas ettirilerek aktarıldı. Laser uygulamaları sürekli dalga ve darbeli şekillerde, farklı süre ve güçlerde (200, 400, 600, ve 800mW) yapıldı. Uygulama süreleri karşılaştırmada kolaylık sağlaması amacıyla her güç seviyesinde 4J'lik enerji dozu verilecek şekilde belirlendi. Laser uygulamalarının ardından dokular H&E ile boyanarak histolojik inceleme sonucunda ablasyon ve toplam değişim alanları değerlendirildi ve ablasyon etkinliği hesaplandı. Çevre dokuların sıcaklığı uygulama alanından 1 mm uzaklıkta dokunun içine yerleştirilen K-tipi bir ısıl-çift kullanılarak ölçüldü ve sıcaklık değişim hızı hesaplandı.

Sıcaklık değişim hızı ile ablasyon bılgeleri arasında güçlü korelasyon görüldü. Hem sürekli dalga hem de darbeli şekillerde yapılan yüksek güç seviyesindeki uygulamalarda daha büyük ablasyon ve toplam değişim alanları elde edilse de ablasyon etkinliğinde önemli bir fark ortaya çıkmadı. Sürekli dalga uygulamalarında darbeli uygulamalara kıyasla daha büyük ablasyon ve toplam değişim alanlarına ve daha yüksek ablasyon etkinliklerine ulaşıldı. Histolojik değerlendirmeyle yüksek güçlü uygulamalarda dar bir kofullaşma alanı ve önemsiz seviyede karbonizasyon gözlemlenmiğtir.

Anahtar Sözcükler: Karaciğer Cerrahisi, Laserin Cerrahisi, Tulyum Fiber Laser, 1940-nm.

TABLE OF CONTENTS

ACKNOWLEDGMENTS . . . iii
ABSTRACT . . . iv
ÖZET . . . v
LIST OF FIGURES . . . viii
LIST OF TABLES . . . x
LIST OF SYMBOLS . . . xi
LIST OF ABBREVIATIONS . . . xii
1. INTRODUCTION . . . 1
1.1 Motivation and Objectives . . . 1
1.2 Outline . . . 3
2. BACKGROUND . . . 4
2.1 The Liver . . . 4
2.1.1 Liver Physiology . . . 4
2.1.2 Liver Anatomy . . . 5
2.1.3 Liver Histology . . . 6
2.1.4 Liver Diseases . . . 7
2.1.4.1 Surgical Liver Diseases . . . 7
2.1.4.2 Liver Resection . . . 9
2.1.4.3 Liver Transplant . . . 9
2.2 Laser Tissue Interactions . . . 11
2.2.1 Photothermal Interactions . . . 13
2.3 Temperature Monitoring Techniques . . . 17
2.4 Therapeutic Applications of Photothermal Interactions . . . 18
2.4.1 Soft Tissue Laser Surgery . . . 18
2.4.1.1 CO_2 . . . 19
2.4.1.2 Nd: YAG . . . 19
2.4.1.3 Diode Lasers . . . 20
2.4.1.4 Thulium Fiber (Tm: Fiber) Laser . . . 20
2.4.2 Liver Laser Therapy and Surgery . . . 23

3. MATERIALS AND METHODS 26
3.1 Samples Collection and Preparation 26
3.2 Laser System and Laser Application Procedure 26
3.2.1 Predosimetry Study 27
3.3 Temperature Measurements 28
3.4 Histological Procedures 30
3.4.1 Tissue Fixation 30
3.4.2 Tissue Processing 31
3.4.3 Paraffin Embedding 32
3.4.4 Microtoming and Slide Preparation 32
3.4.5 Hematoxylin and Eosin Staining (H&E Staining) 33
3.5 Ablation Efficiency and Thermal Damage Evaluation 34
3.6 Data Analysis 35
4. RESULTS 36
4.1 Ablation Area (AA), Total Altered Area (TAA), and Ablation Efficiency (AE) 36
4.1.1 Constant Mode (Continuous-wave) with Different Power Settings . 37
4.1.2 Constant Mode (Pulsed-modulated) with Different Power Settings . 38
4.1.3 Constant Power with Varying Modes 39
4.2 Temperature Measurements 39
4.3 Histological Evaluation 44
5. DISCUSSION 47
5.1 Laser Power 48
5.2 Mode of Operation 49
5.3 Temperature Increase 50
5.4 Tissue Type 52
6. CONCLUSION 54
REFERENCES 56

LIST OF FIGURES

Figure 2.1	Liver Anatomy.	4
Figure 2.2	Liver Histology.	6
Figure 2.3	Light Tissue Interactions.	11
Figure 2.4	Absorption Spectrum of Water and Other Biological Chromophores.	12
Figure 2.5	Map of Laser Tissue Interactions as a Function of Pulse Duration and Laser Power.	13
Figure 2.6	Important Parameters in Photothermal Interaction.	14
Figure 2.7	Critical Temperatures and Durations of Temperatures for Cell Necrosis to Occur.	16
Figure 2.8	Location of Thermal Effects Inside Biological Tissue.	16
Figure 3.1	1940-nm Thulium Fiber Laser System.	27
Figure 3.2	Power Meter (PM 200; Thorlabs Inc., New Jersey, USA).	27
Figure 3.3	Thermoprobe and Thermoprobe Controller.	29
Figure 3.4	Experimental Setup.	29
Figure 3.5	Tissue Blocks Fixed in 10% Formalin.	30
Figure 3.6	Tissues Prepared for Tissue Processing.	31
Figure 3.7	Tissues Embedded in Paraffin Blocks.	32
Figure 3.8	Microtomming and Slide Preparation.	33
Figure 3.9	H&E Stained Tissues.	33
Figure 3.10	A Liver Tissue Exposed to 1940-nm Tm:Fiber Laser at 4X Magnification.	35
Figure 4.1	Mean Ablation Areas (AA), Total Altered Areas (TAA), and Ablation Efficiencies (AE) for the 8 Laser Parameter Combinations Applied.	37
Figure 4.2	Temperature Change for the 8 Laser Parameter Combinations Applied.	40
Figure 4.3	Rate of Temperature Change for the 8 Laser Parameter Combinations Applied.	41
Figure 4.4	Correlation between Rate of Temperature Change and Ablation Area for Continuous-wave Mode.	43

Figure 4.5	Correlation between Rate of Temperature Change and Ablation Area for Pulsed-modulated Mode.	43
Figure 4.6	Distribution of Temperature During and After Laser Radiation.	44
Figure 4.7	Lateral Section of H&E Stained Liver Tissue Induced by 200 mW/c-m at 20 sec (Magnification =4X).	45
Figure 4.8	H&E Stained Liver Tissue Samples Induced by the 8 Laser Parameter Combinations Applied (Magnification =4X).	46

LIST OF TABLES

Table 2.1	Thermal Effects of Laser Radiation.	14
Table 3.1	Laser Parameter Combinations Applied to Liver Tissue.	28
Table 3.2	10 % Formalin Solution.	30
Table 3.3	Tissue Processing Protocol.	31
Table 3.4	H&E Staining Protocol.	34
Table 4.1	Mean Ablation Areas (AA), Total Altered Areas (TAA), and Ablation Efficiencies (AE) for the 8 Laser Parameter Combinations Applied.	36
Table 4.2	Significantly Different Groups for AA, TAA, and AE for Continuous-wave Mode. AA= Ablation Area, TAA= Total Altered Area, AE= Ablation Efficiency.	38
Table 4.3	Significantly Different Groups for AA, TAA, and AE for Pulsed-modulated Mode. AA= Ablation Area, TAA= Total Altered Area, AE= Ablation Efficiency.	38
Table 4.4	Significantly Different Groups for AA, TAA, and AE at Constant Power. AA= Ablation Area, TAA= Total Altered Area, AE= Ablation Efficiency.	39
Table 4.5	Temperature Change and Rate of Temperature Change for the 8 Laser Parameter Combinations Applied.	40
Table 4.6	Significantly Different Groups for Rate of Temperature Change for Continuous-wave Mode.	41
Table 4.7	Significantly Different Groups for Rate of Temperature Change for Pulsed-modulated Mode.	42
Table 4.8	Significantly Different Groups for Rate of Temperature Change at Constant Power.	42

LIST OF SYMBOLS

$^{\circ}$C	Degree Celsius
μ_a	Absorption Coefficient
Δ	Delta

LIST OF ABBREVIATIONS

AA	Ablation Area
AE	Ablation Efficiency
ANOVA	Analysis of Variance
BPO	Benign Prostatic Obstruction
CO_2	Carbon Dioxide
c-m	Continuous-wave Mode
CW	Continuous Wave
ΔT	Temperature Change
ΔT/Time	Rate of Temperature Change
DNA	Deoxyribonucleic Acid
DVT	Deep Vein Thrombosis
ECM	Extracellular Matrix
ENT	Ears, Nose, and Throat
g/min	Grams per Minute
H&E	Hematoxylin and Eosin Stain
HCC	Hepatocellular Carcinoma
Ho: YAG	Hollium-doped Yttrium Aluminum Garnet
IR	Infra-red
J	Joule
LASER	Light Amplification by Stimulated Emission of Radiation
LITT	Laser-induced Interstitial Thermotherapy
ml	Millileter
μm	Micrometer
mm^{-1}	Inverse length (Unit of Absorption Coefficient μ_a)
μs	Microsecond
mW	Milliwatt
Nd: YAG	Neodymium-doped Yttrium Aluminum Garnet
NIR	Near Infra-red

nm	Nanometer
PBS	Phosphate Buffered Saline
p-m-m	Pulsed-modulated Mode
P-value	Probability Value
R	Pearson’s Correlation Coefficient
Sec	Second
St. Sign.	Statistical Significance
TAA	Total Altered Area
ThuVEP	Thulium VapoEnucleation of the prostate
Tm: Fiber	Thulium Fiber
T-test	Tukey Test
W	Watt

1. INTRODUCTION

1.1 Motivation and Objectives

Liver surgery involves different operations on the liver for different diseases. The most common operation performed on the liver is a liver resection. Liver resection is the surgical removal of a portion of the liver, also referred to as partial hepatectomy. It is usually done to remove various types of liver tumors, both benign and malignant (primary or metastatic), that are located in the resected portion of the liver. Liver resection can also be performed on patients with liver cysts.

When considered for the treatment of malignant tumors, the goal of liver resection is to completely remove the tumor with appropriate surrounding margin of normal liver tissue. However, the operation is limited to patients with one or two small (3 cm or less) [1] tumors that have not grown into blood vessels, and with good liver function. Unfortunately, most liver tumors cannot be completely removed because the tumor is in too many different parts of the liver, is too large, or has spread beyond the liver. In addition, most patients with liver tumors usually have other liver problems, mainly cirrhosis. In patients with severe cirrhosis, removing even a small amount of liver tissue at the edges of a tumor might not leave enough liver behind to function appropriately, making liver resection not possible.

Liver transplant is another type of surgery operation of the liver. It is a surgical procedure to remove the whole diseased liver and replace it with either a whole or portion of a healthy liver from a donor. Liver transplant can be an option for those with unresectable tumors, but is restricted to small tumors, and the availability of a liver to be transplanted.

The limited number of patients that can benefit from these conventional surgical therapies, in addition to the possible risks and side effects associated with conventional surgery like bleeding, developing blood clots, and infections, has motivated researches to search for alternative therapies. Alternative therapies include but are not limited to cryotherapy, chem-

ical ablation, electrolysis, and laser therapy.

Laser can induce various effects when applied to tissues. The most important effects are thermal and include tissue coagulation and vaporization. These effects can be employed to achieve different therapeutic outcomes. As an alternative treatment to liver surgery, coagulation can be utilized for the destruction of unresectable tumors, while vaporization can be utilized to remove resectable liver tumors, benign tumors, and cysts. As against conventional surgery where cutting is done with the help of sharp blade, laser can cut and coagulate at the same time offering a bloodless operating field, a no need for sutures , a less operating time, a minimal swelling and scars, and a minimal post operative pain.

Thermal effects of different lasers on soft tissues have been investigated in many scientific studies since the introduction of the first working laser, the Ruby laser in 1962 [2]. As a result, many medical lasers have been developed for different therapeutic procedures. The wavelengths available for soft tissue surgery include CO2, Nd: YAG, Er: YAG, Ho: YAG, diode lasers, and many others. The use of laser as a heat source to destroy liver tumors was first reported by Bown in 1983 [3]. The treatment was referred to as laser-induced thermotherapy, and when performed using fibers, laser-induced interstitial thermotherapy (LITT). LITT is gaining acceptance for the treatment of irresectable liver tumors and as a potential alternative to surgery. The Nd: YAG laser (1064-nm) is currently the most commonly used laser system for LITT. Thulium fiber is chosen for this study because as a fiber laser, it offers several advantages over conventional solid-state lasers including smaller size, higher efficiency, improved spatial beam quality, operation in pulsed or CW mode, and inherent fiber optic beam delivery which enables easy coupling to other fiber optics. The thulium fiber laser used in this study emits at 1940-nm, this offers additional advantage: this wavelength corresponds to one of the absorption peaks of water which is the dominant absorber in tissue in the mid infra-red region, and this means potential for precise cutting and ablation of tissues.

However, and despite the advantages lasers offer, they have a main drawback which is the possible thermal damage of the surrounding tissue which may result in prolonged wound healing. Fortunately this can be minimized by the proper adjustment of laser parameters.

The aim of this thesis is to investigate the ablation efficiency of different working modes and power settings of 1940-nm Thulium fiber laser on liver tissue, in addition to utilizing a real time temperature monitoring to provide the necessary feedback for adjusting the laser parameters to minimize the collateral thermal damage of adjacent tissues.

1.2 Outline

In Chapter 2, background information about liver anatomy, histology, physiology, and liver diseases that require surgical intervention is provided. Laser tissue interaction mechanisms and the biological effects of photothermal interactions are discussed. A literature review of the use of lasers in soft tissue surgery as well as in liver laser-induced thermotherapy and in liver surgery is given.

In Chapter 3, detailed information about the materials used in this study, the laser application procedure, the tissue processing procedure, and the temperature measurement method is given.

In chapter 4, results obtained in this study are listed.

In chapter 5, results of the study are discussed and compared to other studies.

In Chapter 6, conclusion of the study and possible further works are given.

2. BACKGROUND

2.1 The Liver

The liver is the largest internal organ in the body and the second largest organ overall after the skin. It weighs about 1500 grams in the normal adult [4]. It is a reddish brown roughly triangular organ located in the upper right quadrant of the abdomen just beneath the diaphragm with a small portion extending to the upper left quadrant.

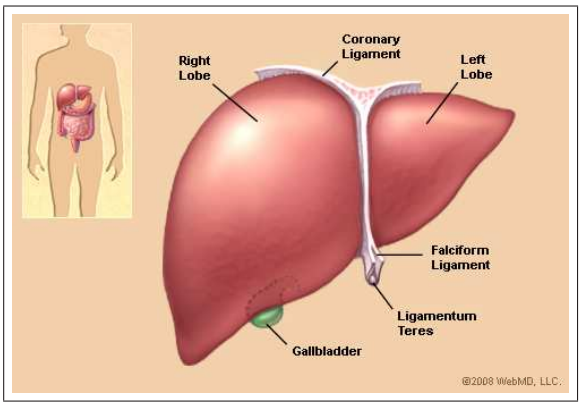

Figure 2.1 Liver Anatomy [5].

2.1.1 Liver Physiology

The liver is also the largest gland in the body. It is considered a gland (a secreting chemicals organ) because it secrets bile which is needed for digestion. In addition to its digestion function, the liver performs many essential functions related to detoxification, metabolism, immunity, and the storage of nutrients within the body. Liver functions include:

- Detoxifying chemicals and metabolizing alcohol and drugs.
- Breaking down hemoglobin as well as insulin and other hormones.

- Producing essential proteins needed for:
  - Blood clotting.
  - Providing resistance to infection.
  - Transporting substances in the blood.
- Storing some vitamins such as vitamin A, and minerals such as iron.
- Storing simple sugar glucose.
- Converting glucose to glycogen to be stored in muscles and liver.
- Manufacturing Cholesterol.
- Converting ammonia to urea.
- Destroying old red blood cells.

These functions make the liver a vital organ. Without a healthy liver, a person cannot survive because the tissues of the body would die from lack of energy and nutrients. Fortunately, the liver is the only organ in the body that has the capability of self regeneration; if part of the liver is removed, the remaining part can grow back to its original size as quickly as a cancerous tumor [6].

2.1.2 Liver Anatomy

The liver is made of very soft reddish-brown tissues enclosed by a thin connective tissue capsule (Glisson's capsule). It is divided into two principal lobes: right and left lobes. The right lobe is about 5 to 6 times larger than the left lobe and they are separated by the Falciform ligament (Figure 2.1). The right lobe is further subdivided into caudate lobe which is the posterior portion of the right lobe, and the quadrate lobe which is on the inferior surface of the right lobe.

The liver has a dual blood supply. The first is the hepatic artery which delivers oxygenated blood from the general circulation to the liver. The second is the hepatic portal vein which delivers nutrients-rich deoxygenated blood from the small intestine to the liver. The blood drains out of the liver via the hepatic veins.

2.1.3 Liver Histology

Histologically, the liver is composed of several components:

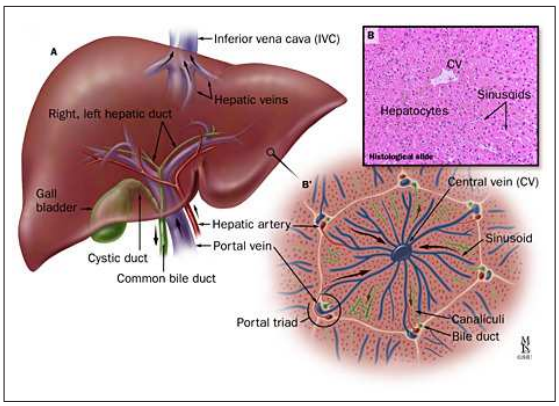

Figure 2.2 Liver Histology [7].

Hepatocytes: These are specialized epithelial cells that make up about 80% of the liver volume [8]. They are the major functional cells in the liver and perform many functions including secretary, metabolic and endocrine functions.

Bile Canaliculi: These are small ducts that collect bile produced by the hepatocytes. From them, the bile passes into bile ductules and then into bile ducts. The bile ducts merge to form the right and left hepatic ducts which constitute the common hepatic duct of the liver which in turn joins the cystic duct from the gallbladder to form the common bile duct that delivers bile to the duodenum.

Hepatic sinusoids: These are small blood vessels between rows of hepatocytes, they receive oxygen-rich blood from the hepatic artery and nutrition-rich deoxygenated blood from the intestines via the portal vein. The hepatic sinusoids converge and deliver blood into a central vein from which the blood flows into hepatic veins which drain into the inferior vena cava.

Portal triad (portal area): The portal triad is composed of branches of hepatic artery, hepatic portal vein, and bile duct.

Lobules: A lobule is a hexagonally shaped functional unit of the liver with portal triads at the vertices and a central vein in the middle from which rows of hepatocytes and hepatic sinusoids are radiating out to the edge of the lobule.

2.1.4 Liver Diseases

Because the liver performs so many essential functions in the body, it is prone to disease. Common diseases of the liver include hepatitis A, B, and C, fatty liver disease, cirrhosis, liver cysts, benign liver masses, and primary and secondary liver cancer. Some diseases can be cured by medications and drugs, while others require surgical intervention.

2.1.4.1 Surgical Liver Diseases. Many liver diseases require surgical intervention. These include:

Liver Cysts

Cysts of the liver can be congenital cysts (present at birth), or acquired cysts which may develop after birth for different reasons such as a traumatic injury. Some people suffer from polycystic liver disease (having many cysts) which is characterized by the liver appearing like a cluster of large grapes. Other people have neoplastic cysts where the liver tissues grow abnormally forming masses that can be either benign or malignant. Cysts can be treated by suction to remove the fluid, but sometimes their removal is required through surgery.

Benign Liver Tumors

The most common benign tumors include hepatocellular adenomas, focal nodular hyperplasia, and cavernous hemangioma. In hepatocellular adenomas, there is a small chance that the tissue could turn cancerous, so removal of the tumor is the best choice. Cavernous hemangioma will never turn into cancerous tissue, but removal of the tumor is required if it is large and causing discomfort. Focal nodular hyperplasia is a very common benign tumor but

it is not known if it can turn into cancerous tumor. In cases where it is difficult to distinguish it from cancerous tumors, removal is the best choice.

Malignant liver Tumors (Liver Cancer)

Malignant liver tumors are divided into primary and secondary malignant liver tumors: Primary malignant liver tumor means that the tumor originated in the liver. This accounts for almost half of all malignant tumors in some undeveloped countries [9]. Secondary malignant liver tumor means that the tumor originated in other parts of the body and spread to the liver (metastatic). The most common malignant tumors that can spread to the liver include colorectal (Bowel), lung, and breast cancers [10].

Primary malignant liver tumors include:

- **Hepatocellular carcinoma:** This is the most common type of primary liver tumors, and probably one of the most common solid cancers in the world [11]. It starts from a hepatocyte which becomes cancerous. Like other cancers, the reasons behind why a cell become cancerous is not known, however, this type of tumor most commonly develops as a complication of liver cirrhosis and Hepatitis B.
- **Cholangiocarcinoma:** This is a cancer of the bile duct system of the liver. It can either develop in the bile duct cells, or in the common bile duct. It is a rare and slow growing type of cancer.
- **Hepatoplastoma:** This type of cancer occurs mainly in children under 5 years of old, however it can occur in older children and adults. It usually develops in the right lobe of the liver and is associated with abnormalities at birth.

Treatments of liver tumors include surgery, chemotherapy, cryotherapy, Alcohol ablation, and radiotherapy. Of these treatments, surgery is the main and the one offering the only reasonable chance to cure liver cancer. Liver surgery can be either a liver resection or a liver transplant.

2.1.4.2 Liver Resection. Liver resection is the surgical removal of portion of the liver which is diseased. It is only possible if the tumor is small and contained in a small part of the liver, and the rest of the liver is healthy. It relies on the liver self regenerating capability. However, in the majority of liver cancer patients, the liver's self regenerative ability is significantly impaired so resection is ruled out as an option. In fact, liver resection has many limitations and complications: it is a major complicated surgery only skillful and experienced surgeons can perform. Because people with liver cancer usually have other liver problems beside the cancer, the surgeon should make a compromise between removing enough of the liver to get rid of the tumor, meanwhile, leaving enough behind for the liver to work properly. This unfortunately results in that most liver cancers cannot be completely removed because the cancer is too large or has spread too far. Possible complications of liver resection include:

- Bleeding; a lot of blood passes through the liver, so bleeding could be a major concern after surgery.
- Developing blood clots in the legs (DVT).
- leaking of bile from the liver. This may require another surgery to stop the leak.
- Infections at the site of surgery.
- Complications from general anesthesia.
- Recurrence of the cancer.
- Pneumonia.
- Liver failure.

In fact, in some cases, liver resection can cause fatal complications such as a heart attack. About 1 out of 30 people who undergo a liver resection will die during or shortly after the operation [12].

2.1.4.3 Liver Transplant. When liver resection is not possible to treat liver tumors for the reasons listed above, a liver transplant can be an option. Liver transplant is a surgical procedure to remove the whole diseased liver and replace it with either a whole or portion of a healthy liver from a donor. Again, Liver transplant is limited to small cases: it can be used on patients with small tumors (either 1 tumor smaller than 5 cm across, or 2 to 3 tumors

no larger than 3 cm) that have not invaded nearby blood vessels. Also it can not be used to treat secondary liver tumor because it originated in some other place than the liver. In addition to that, the opportunities for liver transplants are limited; only about 6,000 livers are available for transplant each year, and most of these are used for patients with diseases other than liver cancer [13]. Away from these limitations or restrictions, liver transplant has also many complications. In fact, in addition to the possible complications associated with a major surgery as indicated in liver resection above, liver transplant can place additional risks including:

- **Liver rejection:** it is common for the immune system to attack the new liver and thus the body rejects the transplanted liver. This occurs in up to 40% of cases, typically in the first 7-14 days after the transplant [14].

Taking this into consideration, a patient undergoing liver transplantation will be given medications (Immunosuppressants) for the rest of her life to help prevent her body from rejecting the transplanted liver. Unfortunately, these medications can cause a variety of risks including:

- Bone thinning
- Diabetes
- Diarrhea
- Headaches
- High blood pressure
- High cholesterol

In attempt to overcome the disadvantages associated with conventional surgery, and the limited number of patients that can undergo this surgery, several alternatives are constantly being developed. One possible alternative is laser surgery. The advantages laser surgery offers over conventional surgery such as bloodless operating field, minimal swelling and scars, and minimal post operative pain made it the subject of many medical research since the first medical laser system was developed and up until now. Currently, many lasers are available

for surgical purposes to treat different medical conditions including cancers.

2.2 Laser Tissue Interactions

The laser light has three unique properties that distinguish it from ordinary light sources: it is monochromatic, directional, and coherent. These properties, in addition to the ability to reach high powers, make it suitable for many applications in manufacturing, metrology, military applications, communications, microscopy, spectroscopy, and medicine [15]. In medicine, the highly focused beam of coherent light offer surgeons the ability to work very precisely to cut, ablate, or coagulate tissues. To achieve the specific task, the mechanism by which laser interacts with tissue should be understood.

When laser light is applied to tissue, and once the laser energy reaches the biological interface, four basic phenomena can take place: absorption, reflection, transmission, and scattering (Figure 2.3). Reflection is usually an undesired effect, and usually only a small fraction of light is reflected and most of laser light penetrates into tissue where it can be transmitted, absorbed, or scattered. This depends on both the optical properties of tissues (absorption, scattering, anisotropy, and refractive index), and on laser parameters.

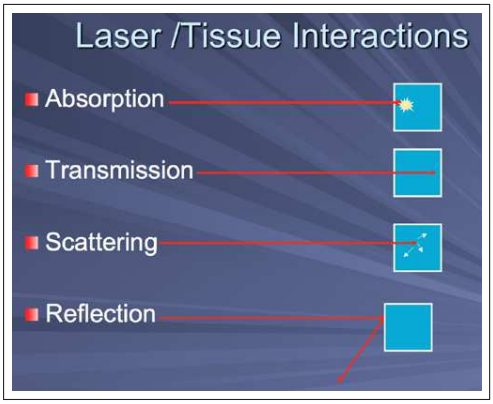

Figure 2.3 Laser Tissue Interactions [16].

Absorption is the most important interaction and it is the key to therapeutic applications. In biological tissues, absorption is caused by chromphores such as water molecules,

proteins, pigments, and other macromolecules. Each wavelength of laser light has specific chromophores that absorb its energy. Thus, selecting a specific laser wavelength depends on the type of lesion being treated and what the main absorber is within it. In the ultraviolet spectral range, DNA and proteins are the main absorbers. In the visible and near infra-red (NIR), hemoglobin and melanin are the main absorbers. Absorption of water, the main constituent of all human tissues (about 65.3%) [17], dominates beyond around 2 μm wavelength. A diagnostic and therapeutic window is defined in the range from 600 - 1200 nm [18]. In this range, light penetrates tissue at a lower loss due to the relatively weak absorption of water and the other chromophores, thus enabling the treatment of deeper tissues. Figure 2.4 shows the wavelength absorption coefficient dependence for some main chromophores in the tissues.

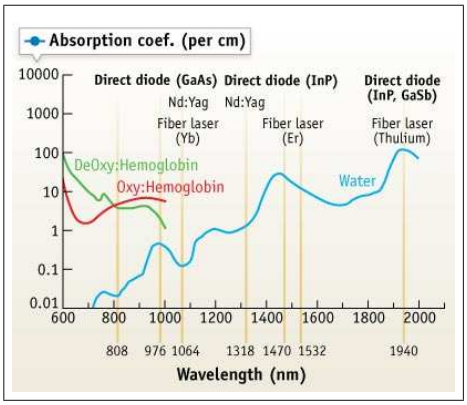

Figure 2.4 Absorption Spectrum of Water and Other Biological Chromophores [19].

Following absorption of laser light, various interaction mechanisms can take place depending on the nature of absorbing tissue, and the laser parameters (wavelength, exposure time, energy density, intensity, power density). Among these, exposure time is the most critical parameter in distinguishing the type of interaction (Figure 2.5). The interaction types can be classified in five main categories: photochemical interactions, photothermal interactions, photoablation, plasma induced ablation, and photodisruption. Photothermal interaction is the most common type utilized in clinical practice.

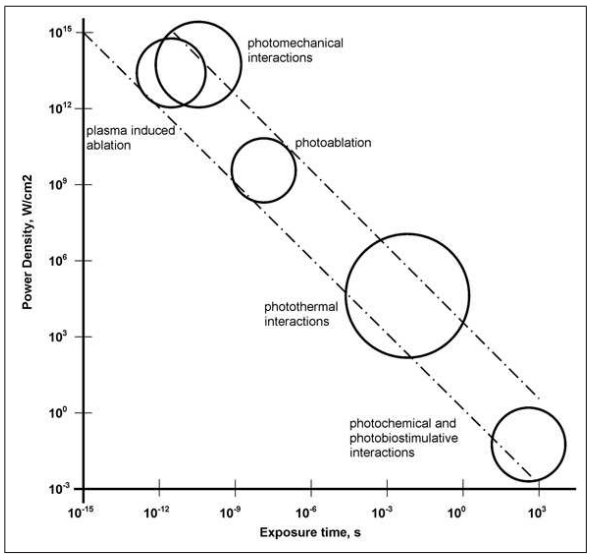

Figure 2.5 Map of Laser Tissue Interactions as a Function of Pulse Duration and Laser Power. (The circles give only a rough estimate of the associated laser parameters) [18].

2.2.1 Photothermal Interactions

Photothermal interactions are probably the most common type of laser tissue interactions encountered in medical procedures. In this type of interaction, the photonic energy is converted into heat energy via molecular vibrations and collisions. Heating a tissue causes a rise in its temperature. The heat will then diffuse through the tissue causing a rise in temperature in the surrounding tissue, and this will result in different thermal effects, the degree and extent of which depends primarily on the magnitude, exposure time, and placement of deposited heat inside the tissue. The deposition of laser energy is a function of laser parameters (wavelength, power density, exposure time, spot size, repetition rate), and optical tissue properties (absorption, scattering). The transfer of energy depends on thermal tissue properties (heat capacity, thermal conductivity). See Figure 2.6.

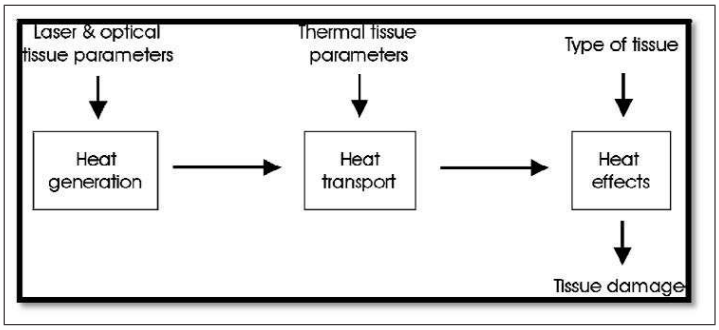

Figure 2.6 Important Parameters in Photothermal Interaction [18].

However, depending on the final temperature reached and the duration of this temperature, different effects can take place: hyperthermia, coagulation, vaporization, ablation, carbonization, and melting (Table 2.1).

Table 2.1
Thermal Effects of Laser Radiation [18].

Temperature	Biological Effect
37°C	Normal
45°C	Hyperthermia
50°C	Reduction in enzyme activity, cell immobility
60°C	Denaturation of proteins and collagen, coagulation
80°C	Permeabilization of membranes
100°C	Vaporization, Thermal decomposition (Ablation)
$>$ 100°C	Carbonization
$>$ 300°C	Melting

With regard to normal body temperature of 37°C, no effects are observed for temperatures up to 42°C.

Hyperthermia refers to the moderate rise in temperature ranging from 42°C to 50°C with an average of 45°C. It is mainly due to conformational changes of molecules in addition to bond destruction and membrane alterations. Hyperthermia usually causes reversible damage. However, if it lasts for several minutes, cell death will result due to changes in enzymatic processes. This effect is usually utilized in laser interstitial thermal therapy (LITT).

Coagulation refers to irreversible cell necrosis without immediate tissue destruction. This is caused by denaturation of proteins and collagen which leads to coagulation of tissue when tissue temperature reaches around 60°C. This effect is often used to seal blood vessels to prevent or stop bleeding by using lasers with wavelengths highly absorbed by hemoglobin. It can also be used to kill malignant tumor cells.

Vaporization occurs when tissue temperatures reaches 100°C. The increase in pressure as water tries to expand in volume as it vaporizes results in localized microexplosions which result in thermal decomposition of tissue fragments. This effect can be utilized to cut and ablate tissue.

Carbonization takes place at temperatures above 100°C. Tissue starts to carbonize releasing carbon which results in blackening of tissue and releasing of smoke. Carbonization is an undesired effect because it reduces visibility during surgical procedures, and has no medical benefits as tissue necrosis is achieved at lower temperatures.

Melting of tissue occurs at high temperatures > 300°C depending on the tissue type.

In fact, it is hard to determine the exact temperature at which cell necrosis begins. In addition to that, it was observed that it is not only the final temperature reached what plays a significant role for the induction of irreversible damage, but also the temporal duration of this temperature. Figure 2.7 illustrates how the critical temperature and the corresponding temporal duration relate to each other for irreversible damage to occur.

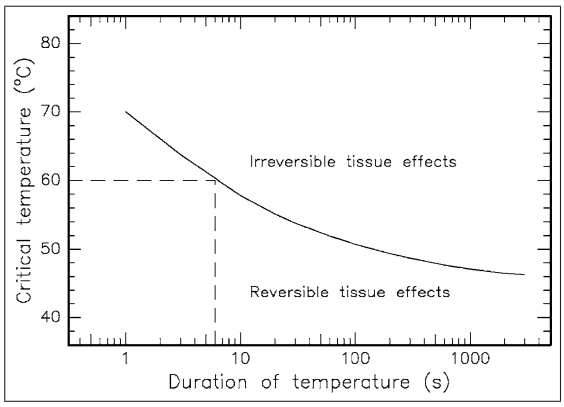

Figure 2.7 Critical Temperatures and Durations of Temperatures for Cell Necrosis to Occur [18].

Most of the time, more than one thermal effect occur in biological tissues depending on the temperature gradient produced in the tissue. Figure 2.8 illustrates the coincidence of several thermal effects. In medical procedures, it is usually one thermal effect that is aimed at, so laser parameters should be chosen very carefully in order to achieve this desirable effect and avoid the others.

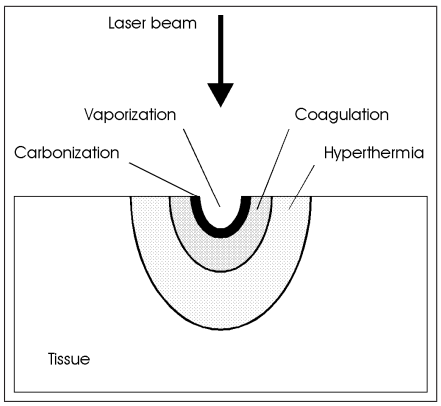

Figure 2.8 Location of Thermal Effects Inside Biological Tissue [18].

However, achieving the desired effect is not the only concern that should be taken into account. Reduction of thermal damage to surrounding tissue to the minimum is of equal concern and a key parameter in determining the success of a laser treatment.

Temperature is certainly the governing parameter of all photothermal interactions. The temperature values reached within tissue and the spatial distribution of this temperature

define the thermal effect and the amount of tissue undergoing thermal damage respectively. Therefore, monitoring temperature increase during laser irradiation of tissue provides a useful feedback to adjust laser parameters to obtain the desired outcome with minimal thermal damage to surrounding healthy tissue.

2.3 Temperature Monitoring Techniques

Different temperature measurement techniques exist. They can be classified into three main categories: point thermometry, surface thermometry, and volumetric thermometry [20]. Each technique has its advantages and disadvantages.

Point (local) Thermometry includes thermocouples and fiber optic sensors. These are widely used due to their simplicity, relatively low cost, wide temperature range, rapid response, and accuracy. However, they have some drawbacks. The main issues are related to their invasiveness. Another drawback related to thermocouples is the overestimation of tissue temperature due to their metallic constitution which directly absorbs laser radiation, and therefore, their measurements require correction [21–23].

In **Surface Thermometry**, temperature of the surface is monitored by thermal sensors such as infra-red cameras [24, 25]. Some of their advantages are their non-invasiveness and the ability to measure temperature over large area. Their disadvantages include their high price, surface-only measurements, and their relatively lower accuracy compared to contact techniques.

In **Volumetric Thermometry**, the temperature at different points within a significant volume is measured. Examples include MRI thermometry and ultrasound thermometry. MRI is more popular due to the high contrast and spatial resolution of its three-dimensional images. Advantages of MRI volumetric thermometry include non-invasiveness, allowing the monitoring of the temperature at the targeted location and in the surrounding tissues, and precision [26, 27]. However they are expensive and more complex than point thermometry.

2.4 Therapeutic Applications of Photothermal Interactions

Ophthalmologists and dermatologists were the first to investigate the biological effects and the possible therapeutic applications of lasers. Just one year after Maiman introduced the first working Ruby Laser in 1960, Leon Goldman, a dermatologist who was later considered the father of laser medicine, demonstrated how the ruby laser could be used to remove port wine stains and melanomas from the skin [28]. In the same year, precisely in December 1961, Dr. Charles J. Campbell of the Institute of Ophthalmology at Columbia-Presbyterian Medical Center and Charles J. Koester of the American Optical Co. at Columbia-Presbyterian Hospital in Manhattan, used a ruby laser on a patient for the first time to destroy a retinal tumor through photocoagulation [29, 30]. Since then, lots of research addressing the potential of laser as a therapeutic tool have taken place. This led to the development of many medical laser systems. As a result, laser treatments found their ways in different fields of medicine: mainly ophthalmology, dermatology, dentistry, oncology, and surgery.

2.4.1 Soft Tissue Laser Surgery

The highly focused, monochromatic, and collimated beam of laser endow lasers with many advantages over conventional surgical techniques such as surgical precision, haemostasis, reduced risk of infection due to bacterial elimination, minimal postoperative scarring, reduced postoperative pain and swelling, and quicker recovery time.

Soft tissue laser surgery is used in a variety of applications in humans including general surgery, oral and maxillofacial surgery, and neurosurgery. Common lasers suitable for soft tissue surgery include CO_2, Nd: YAG, and diode lasers.

Many research investigated the effects of these lasers on different soft tissues for the purpose of developing efficient medical lasers.

2.4.1.1 CO_2. The CO_2 laser was one of the first gas lasers to be developed in 1964 [31]. It is one of the most common and useful lasers used in medicine, and is often referred to as the workhorse for dermatologic and dental lasers. CO_2 laser emits at 10,600 nm which is highly absorbed by water and this makes it very suitable for soft tissues with high water content. The CO_2 can work in continuous wave, pulsed (shuttered continuous-wave), and superpulsed modes. The CO_2 can be used with either a focused beam (0.1 - 0.2 mm) as a light knife for haemostatic tissue incisions, or with a wider unfocused beam (2 - 5 mm) for tissue vaporization [32]. Many studies investigated the potential of CO_2 to cut, vaporize, and coagulate tissues [33–35]. These studies showed that CO_2 offers a reliable tool for cutting and ablating tissues while providing haemostasis. One of the studies [36] showed that CO_2 can produce effective welding to tissues. The effect of laser pulse duration on the residual thermal damage was investigated in studies [37, 38]. The results demonstrated that smaller pulse durations yielded less damage zone than longer pulses and continuous mode. The super pulsed mode appeared also to reduce wound healing delay, a draw back of typical CW CO_2 surgical lasers. Using a 7.5 μs pulse duration , the CO_2 incisions on the dorsal pelts of rats healed with a rate similar to scalpel incisions, and reduced wound healing delay seen with typical CO_2 lasers [39].

2.4.1.2 Nd: YAG. Nd: YAG laser is a solid state laser that was developed in 1964 [40]. It typically emits light with a wavelength of 1064-nm in the near infra-red region, and operates in both continuous-wave and pulsed modes. The low absorption of Nd: YAG laser by tissue chromophores, makes it able to penetrate deeply and cause the coagulation of deep tissues. The high absorption of Nd: YAG in oxyhemoglobin (the main chromophore in dermis) [41] made it suitable to be used in selective photothermolysis, a therapy used in dermatology, and refers to the precise targeting of a structure or tissue using a specific wavelength of light with the intention of absorbing light into that target area alone [42]. As a result, Nd: YAG laser is used to treat many skin disorders such as vascular and pigmented lesions [43–49]. It is also used in laser hair removal. Results showed that it can be used as a safe and effective tool for long-term hair reduction in all skin types [50–53]. It was also shown to be efficient in dark tattoo removal [54–56]. In the last decade the potential of Nd: YAG laser for removing wrinkles was investigated in many studies [57–59]. Away from dermatology, Nd: YAG laser

is also used as a successful therapeutic tool in many other applications such as intraoral surgery [60–62] . The ability of Nd: YAG laser to be coupled with fiber optics made it suitable to be used in laser induced interstitial thermotherapy (LITT). Nd: YAG laser ablation of the prostate as a treatment for benign prostatic hypertrophy was investigated in studies [63] and [64] and yielded effective results.

2.4.1.3 Diode Lasers. Diode lasers are semiconductor lasers. They are valuable and desirable tools in medical applications for a couple of reasons: they can emit continuous or pulsed radiation, they can be coupled with fiber optics, they are extremely compact, and they are cheap. Research has mostly been focused on 810 nm and 980 nm wavelengths due to their high absorption in hemoglobin and water, respectively. Consequently, of the diode lasers currently used, 810 nm and 980 nm lasers are the most common. These lasers have shown a high efficiency in treating many medical situations in ophthalmology, dermatology, dentistry, and others.

The potential of 980 nm diode laser has been investigated in many previous studies for stereotactic brain surgery [65], skin welding [66], intraoral surgery [67], and prostate vaporization [68–70]. Results showed that 980nm can combine high tissue ablative properties with good homeostasis which is due to simultaneous absorption in water and hemoglobin.

810 nm was the research topic of many studies as well. In studies [71,72], its potential as an endovenous laser to treat varicose veins was investigated and the results showed it is effective and safe and can be an alternative to conventional therapies. It was also investigated for the treatment of macular disease [73, 74], and provided satisfactory results.

2.4.1.4 Thulium Fiber (Tm: Fiber) Laser. Thulium doped fiber lasers which operate around 2 μm are emerging as a promising tool for high precision surgical applications for both hard and soft tissues. This is attributed to several aspects: most important is the high absorption in water resulting in short penetration depth in tissue, which translates into efficient tissue ablation accompanied by minimal thermal damage to adjacent healthy tissue.

The second aspect is the coagulation effect of these lasers which provides haemostasis. Another aspect is that these lasers operate in the "eye safe" category ($> 1.4\ \mu$m). They are considered safe for eyes because light in this wavelength range is strongly absorbed in the eye's cornea and lens and therefore cannot reach the more sensitive retina [75]. These aspects in addition to the inherent fiber optic delivery make Tm: fiber lasers ideally suitable for minimally invasive surgical procedures.

The relatively new Tm: fiber laser effects on tissue have been, and still, under investigation by many studies, especially in the field of urology. Most of the studies so far investigated the potential of Tm: fiber laser as an alternative laser lithotripter to the conventional Ho: YAG laser [76–78]. Thermal effects of Tm: fiber laser on soft tissues have also been investigated in other studies including tissue welding of urinary tissues [79], treatment of genital and urethral condylomata acuminata in male patients [80], and resection of the prostate [81, 82]. The efficacy of the CO_2, diode, and CW Thulium laser systems was compared for various clinical applications in ENT, lung and neurosurgery. Tm: fiber laser was shown to be a versatile laser system for a broad range of applications [83].

However, Tm: fiber laser emitting at 1940-nm, the wavelength used in this study, has only been studied in a couple of studies. In one of the studies, Fried et al. investigated the ablation capabilities of a Tm: fiber laser emitting at 1940-nm in urinary tissues in an *in vitro* setting [84]. The study utilized a 40W, CW or pulsed mode laser, used in non contact mode for the vaporization of canine prostate and incision of the animal ureter and bladder neck tissues. Prostate tissue was ablated at a rate of 0.21 ± 0.02 g/min with a thermal coagulation zone of 500 to 2000 μm. Laser incisions of bladder tissue and ureter had coagulation zones of 400 to 600 μm. The results demonstrated Tm: fiber laser has a potential for good haemostasis even in highly vascular tissues such as urinary tissues.

In another study, Theisen-Kunde et al. investigated the potential of 1940nm Tm: fiber for partial kidney resection both *ex vivo* and *in vivo*. Porcine kidneys were used for the study. In the *ex vivo* setting, various velocities and power settings were used in contact mode. Increasing the cutting velocity was shown to decrease the incision depth. Maximum incision depth was obtained at 1 mm/s velocity and 16W power. Coagulation zone was 1 mm

regardless of power or velocity settings used. In the *in vivo* setting, histological examination showed a layer of carbonization of about 100 μm, a layer of coagulation of about 500 to 800 μm. Partial resection of the kidney with 1940-nm laser radiation was shown to be highly sufficient in terms of tissue dissection time and precision with efficient simultaneous haemostasis [85].

Keller et al. assessed the soft tissue ablation performance of 1940-nm Tm: fiber in an *in vitro* study. The laser system operated in either CW or short-pulsed mode at powers ranging from 11 to 20W in contact mode. Different animal tissues were used but detailed results were shown only for chicken breast tissue. Histological evaluation showed a coagulation zone of about 600 μm to 1 mm. A thin carbonization layer was also observed. The results demonstrated that 1940-nm laser system used is highly effective at cutting soft tissues with minimal collateral thermal damage compared with currently used surgical lasers [86].

In another *in vitro* study, Tunç et al. investigated the ablation efficiency of 1940-nm Tm: fiber laser in ovine brain. Powers in the range 200 to 800 mW, delivered in CW and pulsed modes were applied to the brain samples in non-contact mode. It was observed that increasing power values of the Thulium fiber laser resulted in higher ablation and coagulation diameters regardless of delivery mode. Also ablation efficiencies were higher for higher power levels. CW yielded higher mean ablation diameters and higher ablation efficiencies than pulsed mode at the same power [87].

In a recent study, the ablation efficiency of a 1940-nm Thulium fiber laser for intraoral surgery was investigated by Guney et al.. Lamb tongues were used, and the incisions were made in contact mode with a continuous-wave laser at three different speeds, powers, and numbers of passes. Results showed that incision depth and coagulation width both increased with increasing power. Increasing the number of passes at constant speed and power was observed to increase both the incision depth and the coagulation width. Both incision depth and coagulation width increased with decreasing speed. On the whole, high ablation efficiencies were achieved at the lowest speed of 0.5 mm/s. The study showed that 1940-nm Tm: fiber laser can be used to cut with moderate efficiency and produce enough coagulation zone to provide haemostasis [88].

Early postoperative results of the first prospective, randomized comparison of two commercially available thulium lasers: 1940-nm and 2013-nm, for the treatment of benign prostatic obstruction (BPO), using Thulium VapoEnucleation of the prostate (ThuVEP), were demonstrated by Tiburtius et al..The data represented a single center, 30-day short term data. Results showed that 1940-nm and 2013-nm Tm: YAG laser devices are both safe and effective for the mentioned treatment. Both laser devices give satisfactory immediate voiding improvement with low perioperative morbidity [89].

2.4.2 Liver Laser Therapy and Surgery

Several studies were carried out to determine the optical properties of liver tissue. Optical tissue properties (absorption, scattering, anisotropy, and penetration depth) determine light distribution in tissue during laser irradiation which is important for predicting the effects of laser applications and optimizing the clinical implementation of a laser therapy.

Parsa et al. studied the optical properties of a native rat liver between 350 and 2200 nm. Results revealed that the maximum absorption coefficient in the IR region was found at 1940-nm [90].

For Ritz et al., knowing optical properties in the native tissue alone was not enough. Optical properties of tissues are temperature dependent, and therefore, their thermally induced changes during laser irradiation should be determined as well. He studied optical properties of native and coagulated porcine liver tissue between 400 and 2400 nm. He found that in the native tissue, the maximum absorption coefficient of 9.9 mm^{-1}, and the minimum penetration depth of 0.05 mm were found at 1940-nm. Thermal coagulation resulted in a significant increase in the scattering coefficient over the entire spectral range examined. Absorption coefficient and thermal penetration depth decreased after tissue coagulation [91].

The same group had also studied the optical properties of human liver tissue and tissue of colorectal liver metastases at wavelengths of 850-nm, 980-nm and 1,064-nm, and examined the impact of thermal coagulation on these parameters [92]. Results revealed that

liver metastases had a lower absorption and scattering coefficients than healthy liver resulting in a significantly higher optical penetration depth in metastatic tissue. Coagulation resulted in a reduction in the optical penetration depth in both tissue types. Both studies [91, 92] concluded that application parameters should not be kept constant during therapy, but should be adjusted continuously or gradually in order to achieve optimal adaptation to the actual optical penetration depth throughout the application, in order to achieve optimal therapeutic success.

The use of Nd: YAG (1064-nm) laser for laser induced interstitial thermotherapy of the liver was investigated in several animal (*in vitro*, *in vivo*) and clinical studies [93–98]. In fact, Nd: YAG laser is the most used laser so far due to its high penetration depth which can be used to coagulate larger lesions [90–92]. Other lasers studied include diode lasers [99–102] and Holium and Thulium lasers [103, 104].

Ishikawa et al. studied the effect of Nd: YAG (1064-nm) laser system on liver tissue of piglet *in vivo*. He used a fiber with a cone shaped tip. The power, duration, and frequency of irradiation were varied. Histological examination revealed an oval shaped coagulation area in front of the fiber tip. A correlation between coagulation volume and output power was revealed by the results enabling the estimation of coagulation volume based on the laser power applied [97].

The same system was later investigated clinically by Ishikwaw et al. for the treatment of small hepatocellular carcinoma (HCC). Six patients with HCC (mean diameter: 16.3 ± 3.50 mm) underwent the treatment. A laser power of 10W was applied for 10 seconds and repeated three times at a 5-second interval at the targeted tumor in non-contact mode. In all patients, tumor was successfully ablated. Patients were observed for a period of 15 to 26 months, during which no patient died, and no recurrence of HCC in the ablated area was observed for 5 patients [98].

Rohde et al. compared the irradiation effects of Nd: YAG (1064-nm) and diode (940-nm) on porcine liver *in vitro*. Applications were performed in contact mode using a bare fiber with a cooled diffusely scattering applicator. Powers used were in the range 2 to 5W. Results

showed that in the bare fiber experiment, diode laser yielded larger coagulation volumes than Nd: YAG for the same parameters, but carbonization was observed. With the cooled diffusely scattering applicator however, Nd: YAG laser yielded larger coagulation zones. It was reported that with the use of a cooled diffusely scattering applicator, Nd: YAG is more efficient than diode for LITT in liver [101].

Theisen-Kunde et al. investigated the use of 1900-nm Tm: fiber laser for partial liver resection in pig liver *in vivo*. CW laser irradiation at 40W was used in contact mode. After 2-3 weeks, animals were sacrificed, and the healing process of the liver was evaluated by histological analysis. It was reported that during the procedure, hemostasis was highly sufficient that blood loss and bile leakage were negligible. Moderate carbonization of the dissected area was observed. During the survival period no complications such as bleeding or inflammation occurred. Histological examination at the end of survival period showed an ongoing scar formation of about 1 to 2 mm in depth of the dissected area [104].

3. MATERIALS AND METHODS

3.1 Samples Collection and Preparation

Fresh lamb liver specimens were used for the experiments. Immediately after the animal sacrifice, liver specimens were cooled to 4°C as reported by literature [105]. Samples measuring 2X4 cm^2 were cut, washed, and immersed in saline to prevent tissue dehydration. The samples were used within 12 hours of animal sacrifice. Immediately before the experiments, the samples temperature was raised to room temperature between 21 and 23°C. The temperature was measured using a thermocouple. Four laser applications were performed per sample. Applications were spaced apart by 1 cm to allow enough space to avoid boundary effects. A total of 64 laser applications were performed in order to study 8 different laser parameter combinations (power, mode, and exposure) with each parameter combination repeated 8 times.

3.2 Laser System and Laser Application Procedure

Laser irradiations were performed using Thulium fiber laser (TLR-5-1940; IPG Laser GmbH, Germany) that emits at 1940-nm wavelength, can work in continuous-wave mode and modulated (chopped) mode, and has a maximum output power of 5W (Figure 3.1). The term pulsed-modulated mode was used to refer to modulated mode. The laser power was controlled from a screen on the laser device. The laser mode of operation and exposure time were controlled using the custom-built controller unit (Teknofil, Inc., Istanbul, Turkey) that could be accessed through a LabView interface that allows one to specify the ON/OFF duration of pulses and the number of cycles. The output of the laser, which is provided through a 1m fiber optic cable, was coupled to a flat-cut bare-ended optical fiber with a core diameter of 400 μm by means of focusing lenses and XYZ alignment apparatus.

Figure 3.1 1940-nm Thulium Fiber Laser System.

The fiber end was positioned perpendicular to the tissue surface in contact mode (0.5 mm inside the tissue). Before each laser application, the fiber distal end was checked for irregularities and cleaved when necessary. The laser power at that distal end was checked using an optical power-meter (PM 200; Thorlabs Inc., New Jersey, USA), which is shown in Figure 3.2, in order to verify the stability of the laser emission.

Figure 3.2 Power Meter (PM 200; Thorlabs Inc., New Jersey, USA).

3.2.1 Predosimetry Study

In order to determine the laser parameter combinations to be studied, a predosimetry study was needed. It was conducted by exposing liver tissue samples to laser light and observing coagulation and carbonization onsets, and recording them for different power lev-

els starting from 200 mW and increased by small increments of 200 mW. When the power exceeded 800 mW, carbonization was observed consistently. Therefore a range of powers (200 - 800 mW) that can be used safely (i.e., causing no carbonization) was set. Laser exposure times and pulse widths for both continuous-wave mode and pulsed-modulate mode were chosen so that they deliver the same amount of laser energy (4J) to the tissue, so that a convenient comparison between the different laser parameter combinations can be held. Laser parameter combinations used are listed in Table 3.1.

Table 3.1
Laser Parameter Combinations Applied to Liver Tissue.

Laser Power (mW)	Laser mode	Duration(sec)	Laser Energy Delivered (J)
200	c-m	20	4
200	p-m-m	40(100 ms on, 100 ms off)	4
400	c-m	10	4
400	p-m-m	20(100 ms on, 100 ms off)	4
600	c-m	6.7	4
600	p-m-m	13.4(100 ms on, 100 ms off)	4
800	c-m	5	4
800	p-m-m	10(100 ms on, 100 ms off)	4

3.3 Temperature Measurements

Temperature of the nearby tissue was measured using a K-type thermocouple that can detect 0.1°C changes and has a response time of 0.1 sec. The thermocouple was mounted inside a laser thermoprobe system (figure 3.3) developed by our lab and Teknofil Incorporation (based in Istanbul, Turkey) in a previous study [87]. But in this study, it was used as a thermocouple only and the optical fiber was used separately.

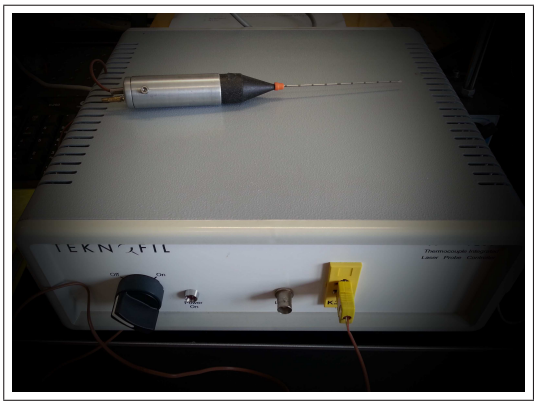

Figure 3.3 Thermoprobe and Thermoprobe Controller.

The thermocouple tip was inserted at a distance of 0.5 mm inside the tissue (at the same level with the fiber tip), and placed 1 mm away from the optical fiber tip (Figure 3.4). Temperature changes were observed real time via a LabView program, that was run on a computer connected to the thermocouple controller.

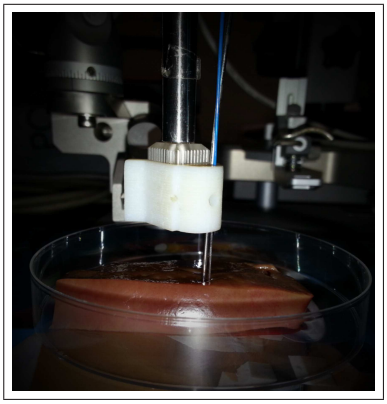

Figure 3.4 Experimental Setup.

3.4 Histological Procedures

3.4.1 Tissue Fixation

Immediately after laser applications, rectangular blocks measuring 1 cm^2 containing the irradiated area surrounded by unaltered tissue were excised and fixed in a 10 % formalin solution at 4°C for 66±6 hours (Figure 3.5). The 10 % formalin solution was prepared as shown in Table 3.2.

Table 3.2
10 % Formalin Solution.

Phosphate Buffered Saline (PBS)	4 Liters
Formaldehyde (37%-40%)	400 ml

Phosphate buffered saline solution was prepared by dissolving tablets of PBS in distilled water. Each tablet was dissolved in 100 ml of distilled water.

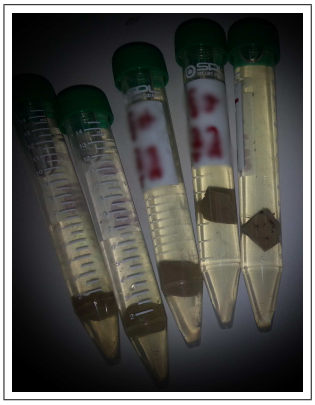

Figure 3.5 Tissue Blocks Fixed in 10% Formalin.

3.4.2 Tissue Processing

At the end of the fixation phase, the blocks were cut laterally at the laser irradiation sites and prepared for tissue processing (Figure 3.6).

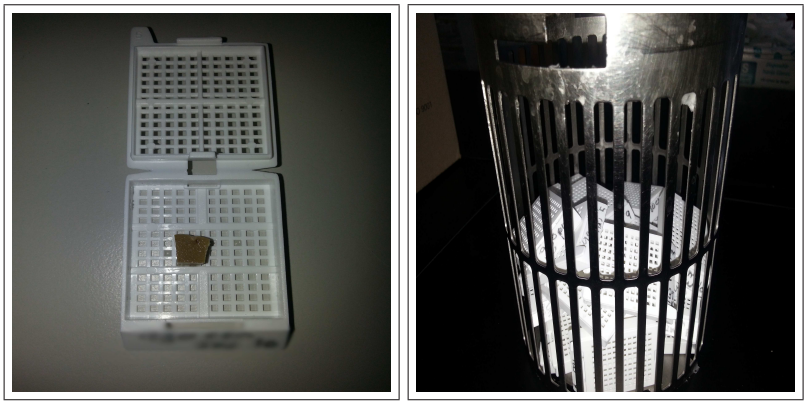

Figure 3.6 Tissues Prepared for Tissue Processing.

Tissue was then processed using tissue processing machine (Lecia TP 1020; Leica Microsystems, Germany) according to the protocol in Table 3.3.

Table 3.3
Tissue Processing Protocol.

Alcohol	70%	30 minutes
Alcohol	80%	30 minutes
Alcohol	80%	30 minutes
Alcohol	96%	30 minutes
Alcohol	96%	30 minutes
Alcohol	100%	30 minutes
Alcohol	100%	30 minutes
Xylene	100%	30 minutes
Xylene	100%	30 minutes
Paraffin	60°C	30 minutes
Paraffin	60°C	30 minutes

3.4.3 Paraffin Embedding

Processed tissues were then embedded in paraffin blocks (Figure 3.7) using the paraffin embedding system (Leica EG1150, Leica Microsystems, Germany). Paraffin blocks were kept at 4°C for one day before being used.

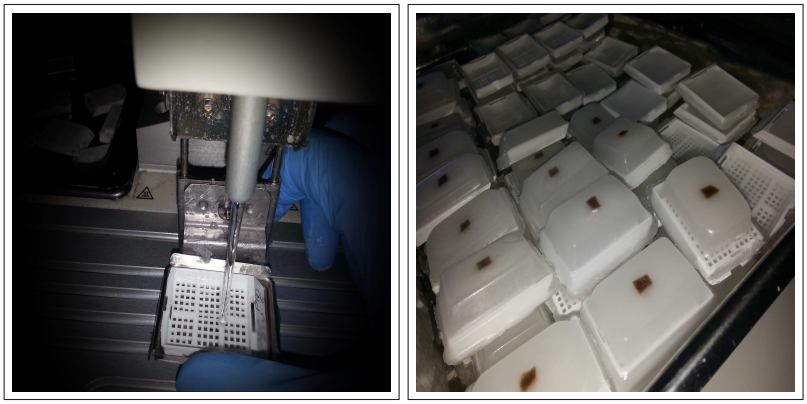

Figure 3.7 Tissues Embedded in Paraffin Blocks.

3.4.4 Microtoming and Slide Preparation

10 μm sections were obtained using a microtome (RM 2255, Leica Microsystems, Germany). Sections were then placed into a 45°C water bath to remove paraffin from over tissue, and then aligned on top of glass slides. Slides were kept overnight in an incubator (Nüve EN 025, Nüve Laboratory and Sterilization Technology, Ankara, turkey) in order to remove remaining paraffin from the tissues (Figure 3.8).

Figure 3.8 Microtomming and Slide Preparation:A: Microtome, B: Water bath, C: Tissues Aligned on Glass Slides.

3.4.5 Hematoxylin and Eosin Staining (H&E Staining)

Tissue sections were then stained with hematoxylin and Eosin (Figure 3.9) using the protocol shown in Table 3.4 to enable visualization of the thermal effects induced by laser irradiation on tissues under light microscopy.

Figure 3.9 H&E Stained Tissues.

Table 3.4
H&E Staining Protocol.

Xylene	7 minutes
Alcohol 100%	2 minutes
Alcohol 90%	2 minutes
Wash in tab water	
Hematoxylene	1.5 minutes
Wash in tab water	
Alcohol 90%	2 minutes
Eosin	2 minutes
Wash in tab water	
Alcohol 90%	2 minutes
Alcohol 90%	2 minutes
Alcohol 100%	2 minutes
Xylene	2 minutes
Dry for 30 seconds	
Cover with Entellan	

3.5 Ablation Efficiency and Thermal Damage Evaluation

Tissue slides were visualized under light microscope (Eclipse 80i; Nikon Co., Tokyo, Japan), and images were captured at two magnifications 4X and 10X. Imaging software (ImageJ; National Institute of health, USA) was used to measure ablated and total thermally altered areas. The total thermally altered area referred to irreversible thermal damage area excluding reversible damaged area (i.e., ablated plus coagulated area). Ablation efficiency was evaluated in terms of a ratio of ablation area to total thermally altered area (Figure 3.10).

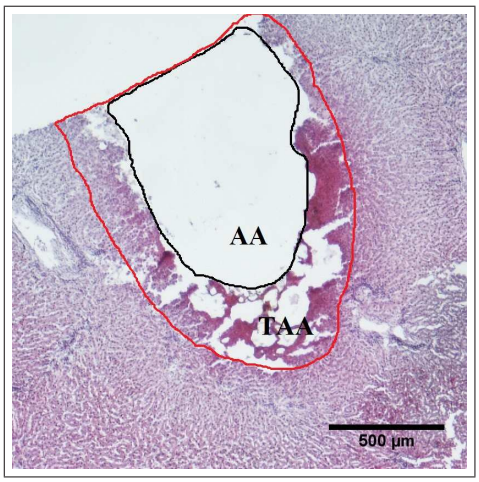

Figure 3.10 A Liver Tissue Exposed to 1940-nm Tm:Fiber Laser at 4X Magnification. AA= Ablation Area, TAA= Total Altered Area.

3.6 Data Analysis

After measurements were obtained for ablated areas, total altered areas, and temperature increases, means and standard deviations of these measurements for each set of laser parameters (obtained from 8 independent samples) were calculated. A 2-way ANOVA was then conducted to reveal the effect of the two parameters (laser power and laser mode) on the ablation and total altered areas as well as on the temperature increases. Tukey test (T-test) was then used as a *post hoc* test to determine the statistical differences between ablated areas, total altered areas, and temperature increases with respect to the two parameters (laser power and laser mode). The significant level was set to $p < 0.05$.

Means and standard deviations for ablation efficiencies and rates of temperature change were also calculated. Pearson's correlation coefficient was used to reveal the relationship between rate of temperature change and ablated and total altered areas.

4. RESULTS

This research focused mainly on investigating the effect of different power and mode settings of 1940-nm Tm: fiber laser on ablation areas, total thermal damage areas, and temperature increases when applied to liver tissue.

4.1 Ablation Area (AA), Total Altered Area (TAA), and Ablation Efficiency (AE)

A 2-way ANOVA revealed that the two parameters (laser power and laser mode) had a significant effect on ablation area and total altered area ($p<0.001$). Regarding ablation efficiency, the effect of laser mode was significant, but the effect of laser power was almost insignificant. The mean values of ablation areas, total altered areas, and ablation efficiencies are shown in Table 4.1, and plotted in Figure 4.1.

Table 4.1
Mean Ablation Areas (AA), Total Altered Areas (TAA), and Ablation Efficiencies (AE) for the 8 Laser Parameter Combinations Applied.

Laser Power (mW)	Laser Mode	AA (mm^2)	TAA (mm^2)	AE %
200	c-m	0.45±0.05	0.71±0.11	63±7
200	p-m-m	0.23±0.05	0.38±0.07	62±4
400	c-m	0.69±0.06	0.92±0.09	75±5
400	p-m-m	0.44±0.05	0.71±0.10	62±6
600	c-m	0.91±0.14	1.29±0.19	71±3
600	p-m-m	0.55±0.04	0.88±0.10	63±5
800	c-m	1.19±0.20	1.63±0.27	73±5
800	p-m-m	0.72±0.10	1.11±0.17	65±2

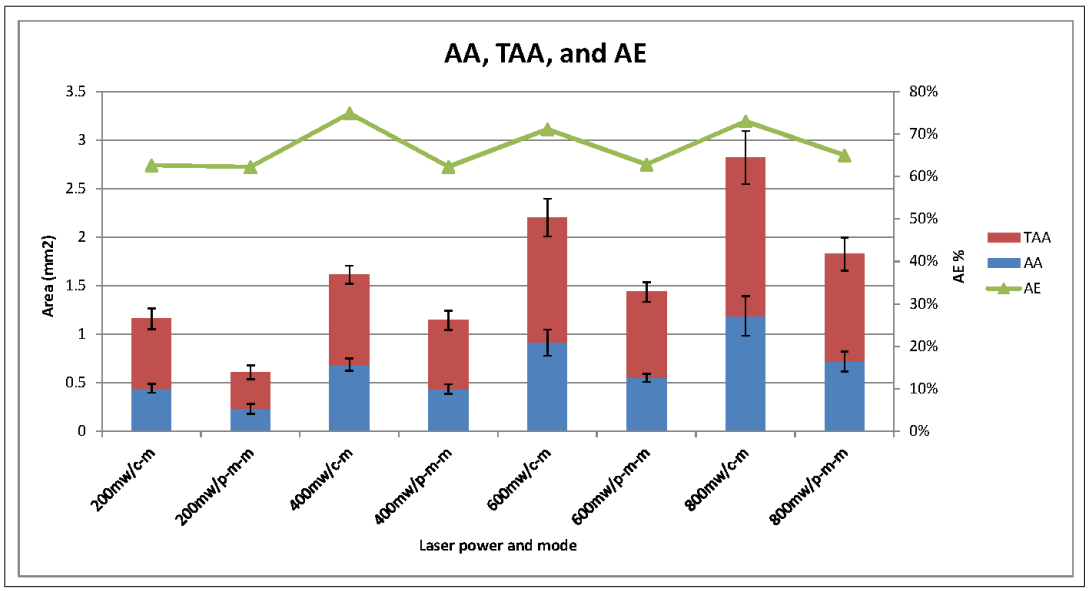

Figure 4.1 Mean Ablation Areas (AA), Total Altered Areas (TAA), and Ablation Efficiencies (AE) for the 8 Laser Parameter Combinations Applied.

The biggest ablation area and total altered area were achieved at 800 mW/c-m. While the highest ablation efficiency of 75% was achieved at 400 mW/c-m. The significant differences in ablation area, total altered area, and ablation efficiency for constant mode (continuous-wave) with varying power settings, constant mode (pulsed-modulated mode) with varying power settings, and constant power with varying modes, are shown in tables 4.2, 4.3, and 4.4 respectively.

4.1.1 Constant Mode (Continuous-wave) with Different Power Settings

As Table 4.2 reveals, for continuous-wave mode, there was a significant difference in ablation area for the different power settings (200, 400, 600, and 800 mW). Increasing the power resulted in higher ablation areas. Total altered area also increased with increasing the power. T-test showed that there was significant difference in TTA between the different power groups except between the power settings 200 mW and 400 mW where there was no significant difference. Regarding ablation efficiency AE, 200 mW resulted in significantly smaller ablation efficiency when compared to 400, 600 , and 800 mW. However, power settings 400, 600, and 800 mW resulted in almost the same ablation efficiencies.

Table 4.2
Significantly Different Groups for AA, TAA, and AE for Continuous-wave Mode. AA= Ablation Area, TAA= Total Altered Area, AE= Ablation Efficiency.

Continuous-wave Mode							
Dependent Variables / Statistical Analysis		AA		TAA		AE	
		P-value	St. Sign.	P-value	St. Sign.	P-value	St. Sign.
ANOVA		0.001	Yes	0.001	Yes	0.001	Yes
T-test Groups	200mw-400mw	0.004	Yes	0.121	No	0.001	Yes
	200mw-600mw	0.001	Yes	0.001	Yes	0.011	Yes
	200mw-800mw	0.001	Yes	0.001	Yes	0.001	Yes
	400mw-600mw	0.008	Yes	0.002	Yes	0.399	No
	400mw-800mw	0.001	Yes	0.001	Yes	0.861	No
	600mw-800mw	0.001	Yes	0.004	Yes	0.850	No

4.1.2 Constant Mode (Pulsed-modulated) with Different Power Settings

For pulsed-modulated mode, increasing the power resulted in significantly higher ablation and total altered areas. However, the effect of laser power on ablation efficiency was not significant. Regardless of the power values, AE was almost the same.

Table 4.3
Significantly Different Groups for AA, TAA, and AE for Pulsed-modulated Mode. AA= Ablation Area, TAA= Total Altered Area, AE= Ablation Efficiency.

Pulsed-modulated Mode							
Dependent variables / Statistical Analysis		AA		TAA		AE	
		P-value	St. Sign.	P-value	St. Sign.	P-value	St. Sign.
ANOVA		0.001	Yes	0.001	Yes	0.578	No
T-test Groups	200mw-400mw	0.001	Yes	0.001	Yes		
	200mw-600mw	0.001	Yes	0.001	Yes		
	200mw-800mw	0.001	Yes	0.001	Yes		
	400mw-600mw	0.009	Yes	0.025	Yes		
	400mw-800mw	0.001	Yes	0.001	Yes		
	600mw-800mw	0.001	Yes	0.003	Yes		

4.1.3 Constant Power with Varying Modes

Changing the mode of laser while keeping the power constant resulted in significantly different values in AA, TAA, and AE for all power values used. Continuous-wave mode produced higher AA, TAA, and AE. The only exception was at 200 mW where there was no significant difference in AE between continuous-wave and pulsed-modulated mode.

Table 4.4
Significantly Different Groups for AA, TAA, and AE at Constant Power. AA= Ablation Area, TAA= Total Altered Area, AE= Ablation Efficiency.

Dependent variables / T- test Groups	AA		TAA		AE	
	P-value	St. Sign.	P-value	St. Sign.	P-value	St. Sign.
200mw(c-m)-200mw(p-m-m)	0.001	Yes	0.001	Yes	0.757	No
400mw(c-m)-400mw(p-m-m)	0.001	Yes	0.001	Yes	0.001	Yes
600mw(c-m)-600mw(p-m-m)	0.001	Yes	0.001	Yes	0.002	Yes
800mw(c-m)-800mw(p-m-m)	0.001	Yes	0.001	Yes	0.001	Yes

4.2 Temperature Measurements

Temperature of the nearby tissue was measured at a distance of 1 mm. For each sample, the maximum temperature rise with respect to the pre-laser temperature (mean = 21°C), the time to reach that maximum, and the rate of temperature change were calculated. Table 4.5 shows mean values of these variables.

Temperature change is plotted in Figure 4.2. The figure shows that the highest temperature increase was achieved at 800 mW/c-m (18.82°C), and the lowest temperature increase was achieved at 200 mW/p-m-m (5.24°C). Increasing the power while keeping the mode constant resulted in higher temperatures. For the same power, continuous-wave mode resulted in higher temperatures when compared to pulsed-modulated mode.

Table 4.5
Temperature Change and Rate of Temperature Change for the 8 Laser Parameter Combinations Applied.

Laser Power (mW)	Laser mode	Temperature change (°C)	Time (sec)	ΔT/Time (°C/sec)
200	c-m	8.12±0.87	20.08±0.42	0.40±0.04
200	p-m-m	5.24±0.36	38.96±0.90	0.13±0.01
400	c-m	11.14±2.20	10.50±1.11	1.10±0.37
400	p-m-m	7.08±0.26	20.16±0.39	0.35±0.02
600	c-m	14.75±1.14	7.05±0.29	2.10±0.21
600	p-m-m	10.42±1.82	13.53±0.24	0.77±0.13
800	c-m	18.82±2.20	5.28±0.27	3.58±0.47
800	p-m-m	11.95±1.32	10.10±0.33	1.19±0.16

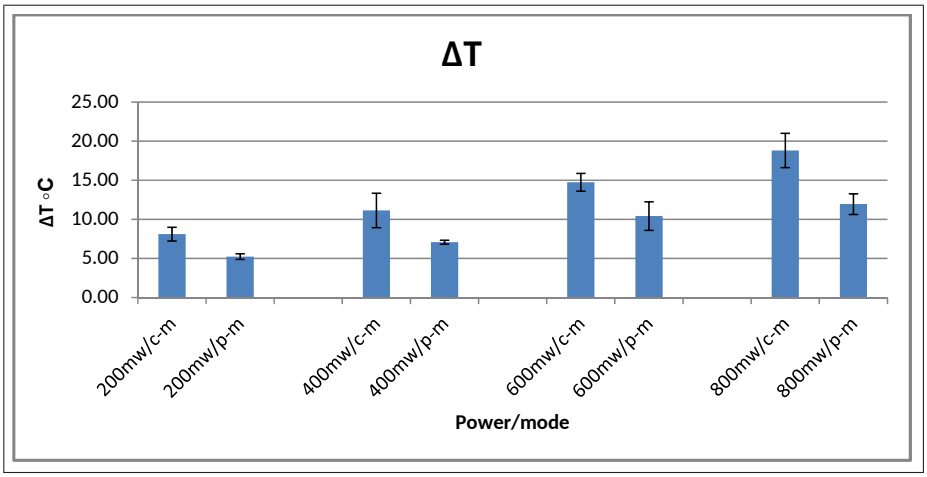

Figure 4.2 Temperature Change for the 8 Laser Parameter Combinations Applied.

The rate of temperature change calculated as the maximum temperature increase divided by the time to reach that maximum, was slowest at 200 mW/p-m-m (0.13±0.01 °C/sec), and fastest at 800 mW/c-m (3.58±0.47 °C/sec). Values are plotted in Figure 4.3.

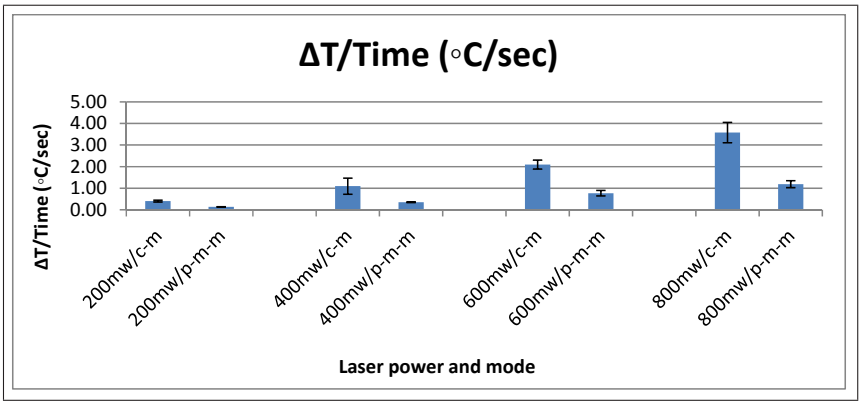

Figure 4.3 Rate of Temperature Change for the 8 Laser Parameter Combinations Applied.

A 2-way ANOVA revealed that the rate of temperature change was differentiated by the two parameters (laser power ($p<0.001$) and laser mode ($p<0.001$)). See Tables 4.6, 4.7, and 4.8.

Increasing the power while keeping the mode constant resulted in higher rates of temperature increase. For the same power, Continuous-wave mode resulted in higher rates of temperature change when compared to pulse-modulated mode.

Table 4.6
Significantly Different Groups for Rate of Temperature Change for Continuous-wave Mode.

Continuous-wave Mode			
Dependent variables / **Statistical Analysis**		**ΔT/Time**	
		P-value	**St. Sign.**
ANOVA		0.001	Yes
T-test Groups	200mw-400mw	0.001	Yes
	200mw-600mw	0.001	Yes
	200mw-800mw	0.001	Yes
	400mw-600mw	0.001	Yes
	400mw-800mw	0.001	Yes
	600mw-800mw	0.001	Yes

Table 4.7
Significantly Different Groups for Rate of Temperature Change for Pulsed-modulated Mode.

Pulsed-modulated Mode			
Dependent variables / Statistical Analysis		ΔT/Time	
		P-value	St. Sign.
ANOVA		0.001	Yes
T-test Groups	200mw-400mw	0.001	Yes
	200mw-600mw	0.001	Yes
	200mw-800mw	0.001	Yes
	400mw-600mw	0.001	Yes
	400mw-800mw	0.001	Yes
	600mw-800mw	0.001	Yes

Table 4.8
Significantly Different Groups for Rate of Temperature Change at Constant Power.

Dependent variables / T- test Groups	ΔT/Time	
	P-value	St. Sign.
200mw(c-m)-200mw(p-m-m)	0.001	Yes
400mw(c-m)-400mw(p-m-m)	0.001	Yes
600mw(c-m)-600mw(p-m-m)	0.001	Yes
800mw(c-m)-800mw(p-m-m)	0.001	Yes

Pearson's correlation coefficient revealed a strong correlation between rate of temperature change and ablation area for both continuous-wave mode (R=0.89), and pulse-modulated mode (R=0.90). Regardless of the laser delivery mode, the higher the rate of temperature change is, the higher the ablation area is. See Figures 4.4 and 4.5.

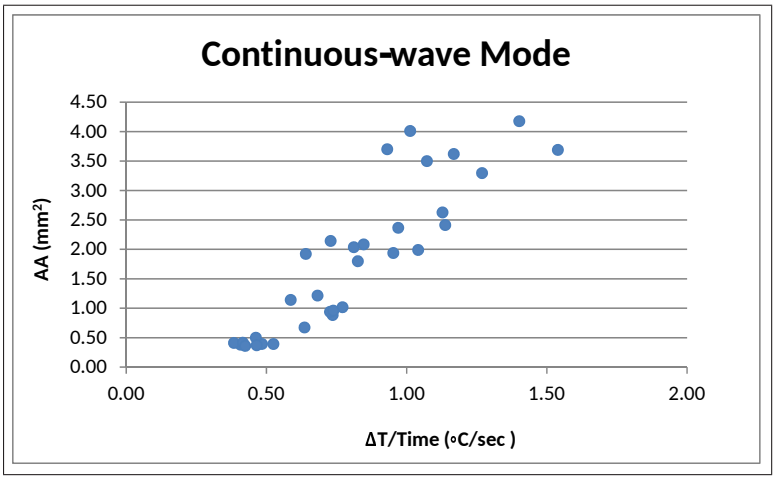

Figure 4.4 Correlation between Rate of Temperature Change and Ablation Area for Continuous-wave Mode.

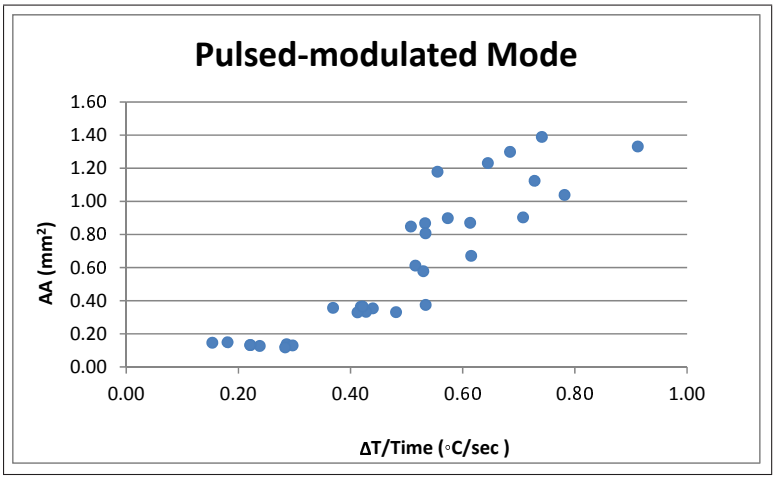

Figure 4.5 Correlation between Rate of Temperature Change and Ablation Area for Pulsed-modulated Mode.

To develop a better understanding of how the temperature of the nearby tissue increased during the time the laser was applied, and later how it decreased after the laser was shut down, a graph showing the distribution of temperature over time was plotted using the mean temperature values measured (10 measurements in a second). This process was repeated for the different laser parameter combinations used. Figure 4.6 shows the results obtained for the 8 laser parameter combinations used. In all applications, Laser was applied at time t= 5sec.

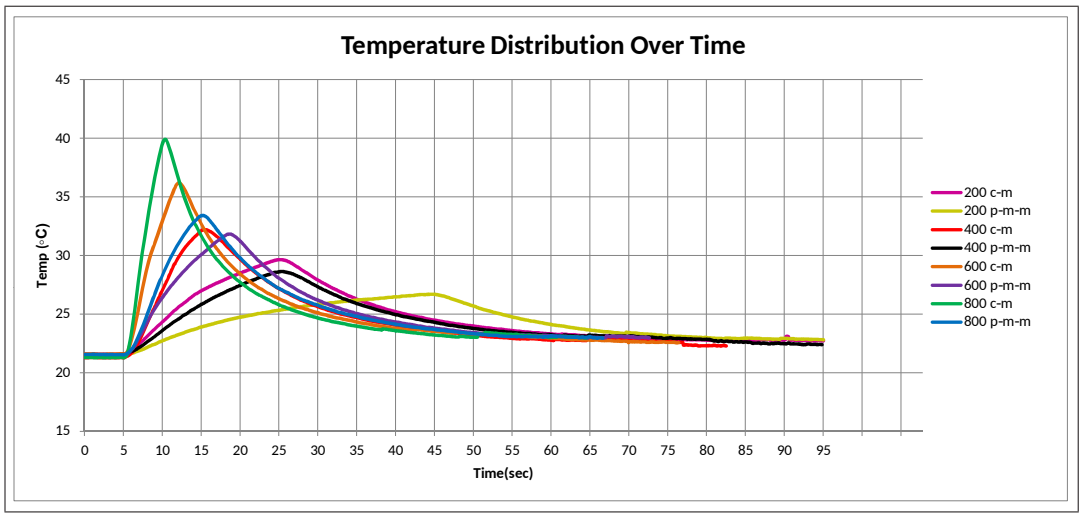

Figure 4.6 Distribution of Temperature During and After Laser Radiation.

A close look at the graph reveals that at 800 mW/c-m and 600 mW/c-m the temperature tended to increase in a linear way. At 800 mW/p-m-m and 400 mw/cm (which had the same exposure time of 10 seconds), the temperature started to increase in a linear way then began to resemble in somehow the shape of a polynomial of the second degree. For the remaining parameter combinations, the temperature increased in a way that can be best fitted with a polynomial of the second degree.

In general, high powers and continuous-wave mode showed a more linear relation when compared to low powers and pulsed-modulated mode.

It can also be seen that the tissue takes a relatively long time to cool down to its pre-laser temperature. During the cooling down, the tissue response was almost similar regardless of the laser delivery mode and power.

4.3 Histological Evaluation

Figure 4.7 shows an example of a H&E stained lateral section induced by 200 mW/c-m at a duration of 20 sec. The slice shows the thermal effects of laser radiation as indexed: (1) ablated area, (2) coagulated area, (3) heat affected area, (4) normal tissue. No signs of

carbonization were visible in this slice. Almost for all the samples, carbonization was not visible. Little signs of tissue carbonization were visible in some of the 800 mW samples but were considered negligible.

An area of heat affected tissue that appeared as lighter tissue was visible in most of the samples. This area was considered as a reversible damage area since nuclei were clearly visible on it. It was not included in calculations of total altered area that was calculated as ablation area plus coagulation area only, i.e., irreversible damage area.

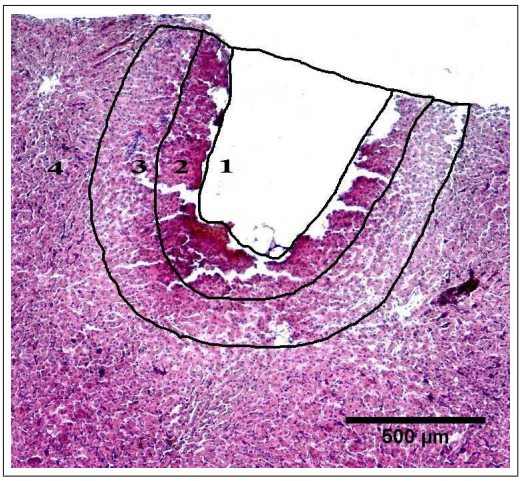

Figure 4.7 Lateral Section of H&E Stained Liver Tissue Induced by 200 mW/c-m at 20 sec (Magnification =4X). Thermal Effects are shown as (1) Ablated Area, (2) Coagulated Area, (3) Heat Affected Area, (4) Normal Tissue.

Examples of H&E stained liver tissue samples that show the thermal effects of the 8 laser parameter combinations applied, are provided in Figure 4.8.

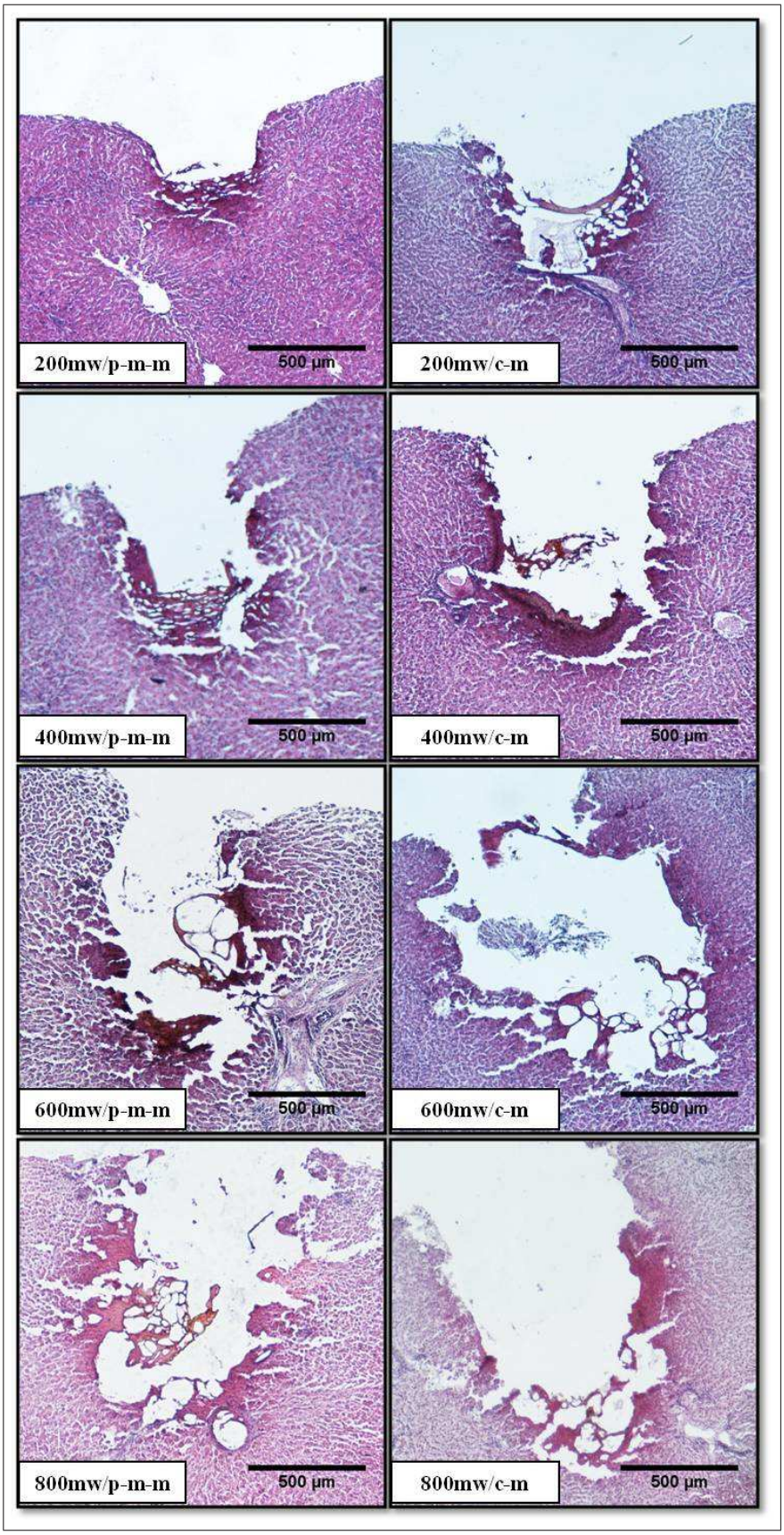

Figure 4.8 H&E Stained Liver Tissue Samples Induced by the 8 Laser Parameter Combinations Applied (Magnification =4X).

5. DISCUSSION

Lasers of wavelengths around 2μm are strongly absorbed by water, the main constituent of biological tissues. Absorption of these wavelengths by a volume of tissue results in a direct and immediate heating of the tissue. This allows for a very precise cutting of the tissue. Furthermore, bleeding during the cutting is repressed by coagulation. This endows the 2μm lasers with a high application potential in surgery and therapy.

The relatively new Tm: fiber laser emitting at 1940-nm, which coincides with one of the absorption peaks of water, was investigated by our laboratory for brain surgery [87], and intraoral surgery [88]. In this study, we proposed the use of Tm: fiber laser as an ablative tool for liver surgery.

To investigate the efficacy of Tm: fiber laser on liver tissue, the ability of the laser to ablate and cut precisely was not our only concern. Minimizing thermal damage to surrounding tissue was as important as well. In order to achieve this, a detailed dosimetry study was carried out to determine the optimal parameters that would lead to the best ablation efficiency with minimal thermal damage. In addition to that, it was taken into account that following absorption of laser light, the tissue temperature increases, which leads to changes in the optical properties of tissues, and thus a change in the absorption coefficient of water (the main chromophore in our study) [106, 107]. These dynamic changes affect the tissue response to laser irradiation [108], and can sometimes reduce the affectivity of even the best dose estimate. To avoid such a situation, a real time temperature monitoring system was utilized in order to better understand mechanisms underlying laser tissue interactions, and to predict the tissue response to laser irradiation. A k-type thermocouple was used for this purpose.

Two different modes and four different laser powers leading to eight different parameter combinations were investigated in this *in vitro* study. For each parameter combination, the ablation area, as well as the total altered area (ablated and coagulated) were measured.

Then ablation efficiency, defined as the ratio of ablated area to total altered area, was calculated to give us an insight on how much tissue was ablated with respect to the total thermal damage produced. Temperature of the nearby tissue was measured at a distance of 1 mm.

Laser irradiation was transferred to the tissue through an optical fiber with a core diameter of 400 μm. The fiber end was positioned perpendicular to the tissue surface in contact mode in order to reduce the amount of reflected light from tissue [109]. Tissues were submerged in saline in order to simulate *in vivo* conditions.

5.1 Laser Power

Ablation area and total altered area both increased with increasing power for both continuous-wave mode and pulsed-modulated mode. This is consisted with previous studies [87, 88, 105, 110]. The increase in both ablation area and total altered area resulted in a similar ablation efficiency (defined as the ratio of ablation area to total altered area) for all power groups in both continuous-wave and pulsed-modulated modes. Only the 200 mW/cm group yielded significantly lower ablation efficiency than the other power groups in continuous-wave mode. In pulsed-modulated mode, there was no significant difference in ablation efficiency between all power groups. Perry et al. reported a similar situation for Nd:YAG laser on oral tissue. He reported that cutting efficiency was not significally improved by increasing power [111].

With a maximum of 75% and a minimum of 62%, all ablation efficiencies achieved were above 50% and were specified as successful by previous study [87]. Ablation efficiencies above 70% can be even specified as highly efficient. The high ablation efficiencies achieved coupled to the fact that the ablation efficiency was independent of the power value used, can be of high advantage. It implies that regardless of the power value used, high ablation will be achieved. So according to the specifications and desired outcomes of the laser intervention such as the size of the area to be ablated, the duration of laser application that should not be exceeded , and the width of coagulation required, the power can be set and a

successful ablation will be achieved.

The effect of power can be depicted in Figure 4.8. Increasing the power resulted in higher ablation areas. It was noticed that ablation depth tended to increase with increasing power more than ablation width, but the overall result was a larger ablation area. Coagulation area also increased with increasing power. Some vacuolization can be seen in the coagulated area. Carbonization was rarely seen .It was only seen for some of the 800 mW samples in a small amount.

5.2 Mode of Operation

It was observed that both ablation area and total altered area increased when changing the mode from pulsed-modulated mode to continuous-wave mode regardless of the power value. However, the increase in ablation area was sharper, and this caused the ablation efficiency to increase significantly between the two modes except at 200 mW where the difference was shown to be insignificant. Indeed, continuous-wave mode was shown to yield a higher ablation than pulsed mode in previous published data [87]. This can be explained by the fact that in continuous-wave mode, the continuous exposure to laser radiation causes the tissue to heat up rapidly resulting in tissue temperatures that can exceed vaporization threshold, so tissue water is removed quickly, and ablation of tissues dominates; more laser energy is consumed in ablation process than in heating nearby tissue, which results in higher ablation efficiencies. In pulsed-modulated mode, the tissue is heated at a slower rate, and during the OFF-period, there is time for the tissue to cool itself and conduct the heat to nearby tissue. So, there is a decrease in the laser energy consumed in ablation process resulting in lower ablation areas which in turn results in lower ablation efficiencies.

The effect of mode can be depicted in Figure 4.8. For the same power, continuous-wave mode yielded deeper ablation and wider coagulation than pulsed-modulated mode. But the increase in coagulation was less than the increase in ablation area resulting in higher ablation efficiencies for continuous-wave mode.

5.3 Temperature Increase

Our results revealed that there was a strong correlation between rate of temperature change and ablation area. A fast and sudden increase in temperature resulted in higher ablation areas, with the highest rate of temperature change of 3.58±0.47 °C/sec corresponding to the highest ablation area of 1.19±0.20 mm^2 achieved at 800 mW/c-m. Whereas, a slow and prolonged rate of increase of temperature resulted in lower ablation areas, with the slowest rate of 0.13±0.01 °C/sec corresponding to the lowest ablation area of 0.23±0.05 mm^2 achieved at 200 mW/p-m-m.

A strong correlation was also revealed between rate of temperature change and total altered area. Higher total altered areas also corresponded to higher rates of temperature change and vice versa.

This dual correlation between both ablation area and total altered area with rate of temperature change, resulted in a weak correlation between rate of temperature change and ablation efficiency (R=0.43, R=0.27) for continuous-wave mode and pulsed-modulated mode, respectively.

This high correlation between the rate of temperature change and ablation and total altered areas, implies that the real time temperature system utilized in this study serves an important mean to predict thermally irreversible damage areas and avoid carbonization which is of great medical concern in laser assisted surgery.

Higher powers and continuous-wave mode yielded higher temperature peaks and rates of temperature change than lower powers and pulsed-modulated mode, which is consisted with previous studies [87, 111, 112].

Looking back at Table 4.5, the range of temperature increase was from 5.24 to 18.82 °C. These values should be considered in light of the measurement system. There are two aspects that tend to have opposite effects on the measurements: one tends to overestimate the results, and the other tends to underestimates the results.

The first aspect is related to the metallic constitution of the thermocouple. The metal conductors of the thermocouple absorb laser radiation and cause a local and instantaneous increase in temperature which entails an overestimation of the actual temperatures measured [21,23]. Solution to this artifact was suggested in different studies [21–23,113] . Anvari et al. suggested splitting the temperature increase into two parts: one with shorter response time which is caused by this artifact, and the other with the longer response time which is caused by the tissue temperature increase [23]. Then this artifact can be corrected by subtracting this sudden increase or decrease in temperature which happens when the laser is turned on or off respectively [21] . In our study, the thermocouple was inserted 0.5 mm inside the tissue to make sure that it was surrounded by tissue from all the sides to minimize this artifact. Presence of a sudden increase or decrease in temperature when the laser was turned on or off was not visible. See Figure 4.6.

The second aspect is the time response of the temperature measurement system. In our study it was 0.1 sec, which is much slower than the thermal response of the tissue to laser irradiation which is in the nanosecond level as reported previously [87, 114]. Ishihara et al. showed that for the same laser fluence, a dramatic difference in the results measured between measurement systems with thermal responses in the nanosecond and microsecond was found [114]. So, for more accurate estimation of the real tissue temperature a measurement system with a faster response time is suggested to be used.

However, the temperature of nearby tissue as measured by our system served as a good means to point out the photothermal effect, and this was revealed by the strong correlation between rate of temperature increase and ablated and total altered areas.

5.4 Tissue Type

Comparing the results obtained in this study on liver tissue with results obtained in a previous study on brain tissue [87], which used the same laser parameters exactly (applied energy, laser powers, and exposure times), revealed that liver tissue yielded higher ablation efficiencies than brain tissue for all laser parameter combinations used. A statistical analysis was not carried out to determine if there was a significant difference in the results or not. However, differences in optical properties of liver and brain tissue which depend on the tissue constituents, and the concentration of chromophores can yield differences in their response to laser light. Both liver and brain have high water content of about 78% [115, 116], but they differ in other tissue constituents. Although there is no published data for the optical properties of brain tissue at 1940-nm (for liver tissue there is [90, 91]), but for other wavelengths, previous studies revealed that liver tissue has higher absorption coefficient than brain tissue and other soft tissues [117, 118]. This is expected to be the case for 1940-nm as well, and can explain the higher ablation efficiency related to liver tissue.

There was also a difference in the tissue response to pulsed-modulated mode regarding temperature increases. For liver tissue, pulsed-modulated mode yielded less temperature increase than continuous-wave mode for the same power value, while for brain tissue , pulsed-modulated mode yielded higher temperature increase than continuous-wave mode for the same power value except for low power of 200 mW. Tissue response to pulsed laser radiation is influenced by the ratio of laser pulse duration to thermal relaxation time which is a function of thermal diffusivity [119], and hence depends on the thermal properties of the tissue. This may account for the reported difference mentioned.

In fact, the composition and morphology of liver tissue make it suitable for laser ablation. The extracellular matrix (ECM) fraction of the liver is quite small and consists mainly of cell adhesion proteins with low collagen content [115, 119]. One of the primary functions of ECM is to maintain the structural integrity of the tissue, and hence it inhibits tissue vaporization and material removal. This means that liver tissue can be easily ablated.

This extremely cellular nature and low connective tissue content of the liver , which

make it so friable and easily torn, also explains the little tearing of liver tissue that was observed and can be noticed in Figure 4.8.

It should be mentioned that this study was performed on normal liver tissue only. The difference in thermal and optical properties between normal and tumor tissue may influence the mechanisms by which tissue is heated , and therefore, the effect of Tm: fiber laser on tumor liver tissue may vary [92,120]. Further experiments should be carried out to investigate the effect of Tm: fiber laser on tumor liver tissue.

6. CONCLUSION

The aim of this study was to investigate the potential of 1940-nm Tm: fiber laser as an ablative tool for liver surgery. This was done by investigating the ablation capability of different working modes and power settings of 1940-nm Tm: fiber laser on liver tissue, with utilizing a real time temperature monitoring system to provide the necessary feedback for adjusting the laser parameters to minimize the collateral thermal damage to adjacent tissues in an *ex vivo* setting.

This study showed that with a proper selection of laser parameters such as laser power, laser mode of operation, and exposure time, the efficiency of a laser system can be improved. The results obtained revealed a high ablation capability of the 1940-nm Tm: fiber laser for use on liver tissue. With only low laser powers of less than 1W, high ablation efficiencies of more than 70% were obtained, and a suitable coagulation zone which is needed to provide hemostasis was produced. Furthermore, the real time temperature measurement of the nearby tissue served as a good pointer to the photothermal effects, which can be used to confine thermal damage to surrounding tissue and prevent unwanted effects such as carbonization.

The results obtained in this study are encouraging. However, they should be considered in light of the limitations of *ex vivo* studies. Although some steps were taken to simulate *in vivo* conditions such as the use of fresh samples, and immersion in saline, but loss of perfusion in *ex vivo* studies means loss of chromphores which may influence performance of the laser system. Blood perfusion can provide a cooling effect under *in vivo* conditions which can affect the thermal response of the tissue to the applied laser irradiation; smaller ablation areas and less temperature increases are expected compared to *ex vivo*.

Further investigation of the potential of 1940-nm Tm: fiber laser in *in vivo* studies must be carried out before it can be proposed for clinical use. Should the high ablation capability and sufficient coagulation needed for hemostasis as revealed by this study be confirmed

in *in vivo* studies, the 1940-nm Tm: fiber laser can be introduced as a promising tool with high potential for laser assisted liver surgery.

REFERENCES

1. *liver Resection*, MedicineNet. Available: http://www.medicinenet.com/liver_resection/article.htm.
2. Townes, C. H., *How the Laser Happened: Adventures of a Scientist*, New York: Oxford University Press, Inc., 1999.
3. Bown, S. G. M., "Phototherapy of tumors," *World Journal of Surgery*, Vol. 7, no. 6, pp. 700–709, 1983.
4. Longmire, W. P., and Tompkins, R. K., *Manual of Liver Surgery*, New York: Springer Science, 1981.
5. *Picture of the Liver*, WebMD. Available: http://www.webmd.com/digestive-disorders/picture-of-the-liver.
6. *Liver*, InnerBody. Available: http://www.innerbody.com/image_digeov/card10-new2.htmlfull-description.
7. *Hepatocellular Carcinoma (Liver Cancer): Anatomy*, Johns Hopkins Medicine. Available: https://gi.jhsps.org/GDL_Disease.aspx?CurrentUDV=31&GDL_Cat_ID=BB532D8A-43CB-416C-9FD2-A07AC6426961&GDL_Disease_ID=A349F0EC-5C87-4A52-9F2E-69AFDB80C3D1.
8. Tortora, G. J., and Derrickson, B. H., *Principles of Anatomy and Physiology*, USA: John Wiley & Sons, Inc., 12 ed., 2008.
9. *Understanding Liver Cancer – the Basics*, WebMD. Available: http://www.webmd.com/cancer/understanding-liver-cancer-basic-information.
10. *Secondary Cancer in the Liver*, Cancer Research UK. Available: http://www.cancerresearchuk.org/about-cancer/type/secondary-cancers/secondary-liver-cancer/secondary-liver-cancer.
11. Curley, S. A., *Liver Cancer*, New York: Springer Science, 1998.
12. *Liver Cancer - Treatment*. Available: http://www.nhs.uk/Conditions/Cancer-of-the-liver/Pages/Treatment.aspx.
13. *Liver Cancer Surgery*, American Cancer Society. Available: http://www.cancer.org/cancer/livercancer/detailedguide/liver-cancer-treating-surgery.
14. *Liver Transplant - Complications*. Available: http://www.nhs.uk/Conditions/Liver-transplant/Pages/Complications.aspx.
15. *Laser Applications*, RP Photonics Encyclopedia. Available: http://www.rp-photonics.com/laser_applications.html.
16. *Laser Tissue Interactions and Biological Effects*. Available: http://www.dentalcare.com/en-US/dental-education/continuing-education/ce394/ce394.aspx?ModuleName=coursecontent&PartID=3&SectionID=-1.
17. Duck, F. A., *Physical properties of tissues: a comprehensive reference book*, London: Academic Press Limited, 1990.

18. Niemz, M. H., *Laser- Tissue Interactions: Fundamentals and Applications*, New York: Springer, 2007.

19. *Bright laser diodes combat cancer*. Available: http://www.bioopticsworld.com/articles/2009/07/bright-laser-diodes-combat-cancer.html.

20. Sajjadi, A. Y., Mitra, K., and Guo, Z., "Thermal Analysis and Experiments of Laser-Tissue Interactions: A Review," *Heat Transfer Research*, Vol. 44, no. 3-4, pp. 345–388, 2013.

21. Saccomandi, P., Schena, E., and Silvestri, S., "Techniques for temperature monitoring during laser-induced thermotherapy: An overview," *International Journal of Hyperthermia*, Vol. 29, no. 7, pp. 609–619, 2013.

22. Manns, F., Milne, P. J., Gonzalez-Cirre, X., Denham, D. B., Parel, J.-M., and Robinson, D. S., "In situ temperature measurements with thermocouple probes during laser interstitial thermotherapy (LITT): Quantification and correction of a measurement artifact," *Lasers in Surgery and Medicine*, Vol. 23, no. 2, pp. 94–103, 1998.

23. Anvari, B., Motamedi, M., Torres, J. H., Rastegar, S., and Orihuela, E., "Effects of surface irrigation on the thermal response of tissue during laser irradiation," *Lasers in Surgery and Medicine*, Vol. 14, no. 4, pp. 386–395, 1994.

24. Launay, Y., Mordon, S., Cornil, A., Brunetaud, J. M., and Moschetto, Y., "Thermal effects of lasers on dental tissues," *Lasers in Surgery and Medicine*, Vol. 7, no. 6, pp. 473–477, 1987.

25. Torres, J. H., Springer, T. A., Welch, A. J., and Pearce, J. A., "Limitations of a thermal camera in measuring surface temperature of laser-irradiated tissues," *Lasers in Surgery and Medicine*, Vol. 10, no. 6, pp. 510–523, 1990.

26. Dibaji, S. A. R., Wansapura, J., Myers, M. R., and Banerjee, R. K., "In Vivo Monitoring of HIFU Induced Temperature Rise in Porcine Liver Using Magnetic Resonance Thermometry," *Journal of Medical Devices*, Vol. 8, no. 3, 2014.

27. Quesson, B., Laurent, C., Maclair, G., de Senneville, B. D., Mougenot, C., Ries, M., Carteret, T., Rullier, A., and Moonen, C. T., "Real-time volumetric MRI thermometry of focused ultrasound ablation in vivo: a feasibility study in pig liver and kidney," *NMR in Biomedicine*, Vol. 24, no. 2, pp. 145–153, 2011.

28. Harris, S., "Lasers in Medicine," *SPIE Professional*, January 2011.

29. Spetz, J., "Physicians and Physicists: The Interdisciplinary Introduction of the Laser to Medicine," in *Sources of Medical Technology: Universities and Industry* (Rosenberg, N., Gelijns, A. C., and Dawkins, H., eds.), ch. 3, pp. 41–66, National Academies Press (US), 1995. Available: http://www.ncbi.nlm.nih.gov/books/NBK232041/?report=reader.

30. Rose, M., "A History of The Laser: A Trip Through The Light Fantastic," *Photonics Spectra*, May 2010.

31. Patel, C. K. N., "Continuous-Wave Laser Action on Vibrational-Rotational Transitions of CO_2," *Phys. Rev.*, Vol. 136, no. 5A, pp. A1187–A1193, 1964.

32. Fitzpatrick, R. E. M., and Goldman, M. P. M., "Advances in carbon dioxide laser surgery," *Clinics in Dermatology*, Vol. 13, no. 1, pp. 35–47, 1995.

33. Pick, R. M., and Pecaro, B. C., "Use of the CO_2 laser in soft tissue dental surgery," *Lasers in Surgery and Medicine*, Vol. 7, no. 2, pp. 207–213, 1987.

34. Barak, S., and Kaplan, I., "The CO_2 laser in the excision of gingival hyperplasia caused by nifedipine," *Journal of Clinical Periodontology*, Vol. 15, pp. 633–635, Nov 1988.

35. Christenson, L. J., Smith, K., and Arpey, C., "Treatment of Multiple Cutaneous Leiomyomas with CO_2 Laser Ablation," *Dermatologic Surgery*, Vol. 26, pp. 319–322, April 2000.

36. Lobel, B., Eyal, O., Kariv, N., and Katzir, A., "Temperature controlled CO_2 laser welding of soft tissues: Urinary bladder welding in different animal models (rats, rabbits, and cats)," *Lasers in Surgery and Medicine*, Vol. 26, no. 1, pp. 4–12, 2000.

37. Walsh., J. T., Flotte, T. J., Anderson, R. R., and Deutsch, T. F., "Pulsed CO_2 laser tissue ablation: Effect of tissue type and pulse duration on thermal damage," *Lasers in Surgery and Medicine*, Vol. 8, no. 2, pp. 108–118, 1988.

38. Ross, E. V., Domankevitz, Y., Skrobal, M., and Anderson, R. R., "Effects of CO_2 laser pulse duration in ablation and residual thermal damage: Implications for skin resurfacing," *Lasers in Surgery and Medicine*, Vol. 19, no. 2, pp. 123–129, 1996.

39. Sanders, D. L., and Reinisch, L., "Wound healing and collagen thermal damage in 7.5-μsec pulsed CO_2 laser skin incisions," *Lasers in Surgery and Medicine*, Vol. 26, no. 1, pp. 22–32, 2000.

40. Fisher, J. C., "A Brief History of the Nd: YAG Laser," in *Advances in Nd: YAG Laser Surgery* (Joffe, S. N., and Oguro, Y., eds.), pp. 7–9, New York: Springer, 1988.

41. Green, J., and Kaufman, J., "Long-pulsed 1,064 nm Nd: YAG lasers effective in vein, PWS, other treatments," *Dermatology Times*, March 2012. Available: http://dermatologytimes.modernmedicine.com/dermatology-times/news/modernmedicine/modern-medicine-now/long-pulsed-1064-nm-ndyag-lasers-effective?page=full.

42. *Selective Photothermolysis Definition*. Available: http://plasticsurgery.about.com/od/glossary/g/selective_PTL.htm.

43. Landthaler, M., Haina, D., Brunner, R., Waidelich, W., and Braun-Falco, O., "Neodymium-YAG laser therapy for vascular lesions," *Journal of the American Academy of Dermatology*, Vol. 14, no. 1, pp. 107–117, 1986.

44. Rosenfeld, H., and Sherman, R., "Treatment of cutaneous and deep vascular lesions with the Nd: YAG laser," *Lasers in Surgery and Medicine*, Vol. 6, no. 1, pp. 20–23, 1986.

45. Anderson, R. R., Margolis, R. J., Watenabe, S., Flotte, T., Hruza, G. J., and Dover, J. S., "Selective Photothermolysis of Cutaneous Pigmentation by Q-switched Nd: YAG Laser Pulses at 1064, 532 and 355 nm," *Journal of Investigative Dermatology*, Vol. 93, no. 1, pp. 28–32, 1989.

46. TSE, Y., LEVINE, V. J., MCCLAIN, S. A., and ASHINOFF, R., "The Removal of Cutaneous Pigmented Lesions with the Q-switched Ruby Laser and the Q-switched Neodymium: Yttrium-Aluminum-Garnet Laser," *The Journal of Dermatologic Surgery and Oncology*, Vol. 20, pp. 795–800, Dec 1994.

47. Goldberg, D. J., "Laser Treatment Of Pigmented Lesions," *Dermatologic Clinics*, Vol. 15, pp. 397–407, July 1997.

48. Weiss, R. A., and Weiss, M. A., "Early Clinical Results with a Multiple Synchronized Pulse 1064 NM Laser for Leg Telangiectasias and Reticular Veins," *Dermatologic Surgery*, Vol. 25, pp. 399–402, May 1999.

49. Yang, M. U., Yaroslavsky, A. N., Farinellia, W. A., Flotte, T., Rius-Diaz, F., Tsao, S. S., and Anderson, R. R., "Long-pulsed neodymium:yttrium-aluminum-garnet laser treatment for port-wine stains," *Journal of the American Academy of Dermatology*, Vol. 52, no. 3, pp. 480–490, 2005.

50. Bencini, P. L., Luci, A., Galimberti, M., and Ferranti, G., "Long-term Epilation with Long-Pulsed Neodimium:YAG Laser," *Dermatologic Surgery*, Vol. 25, no. 3, pp. 175–178, 1999.

51. Fournier, N., Aghajan-Nouri, N., Barneon, G., and Mordon, S., "Hair removal with an Athos Nd: YAG 3.5 ms pulse laser: a 3-month clinical study," *Journal of Cosmetic and Laser Therapy*, Vol. 2, no. 3, pp. 125–130, 2000.

52. Alster, T. S., Bryan, H., and Williams, C. M., "Long-pulsed Nd: YAG laser-assisted hair removal in pigmented skin: a clinical and histological evaluation," *Archives of Dermatology*, Vol. 137, no. 7, pp. 885–889, 2001.

53. Tanzi, E. L., and Alster, T. S., "Long-Pulsed 1064-nm Nd: YAG Laser-Assisted Hair Removal in All Skin Types," *Dermatologic Surgery*, Vol. 30, no. 1, pp. 13–17, 2004.

54. Kilmer, S. L., and Anderson, R. R., "Clinical Use of the Q-Switched Ruby and the Q-Switched Nd: YAG (1064 nm and 532 nm) Lasers for Treatment of Tattoos," *The Journal of Dermatologic Surgery and Oncology*, Vol. 19, no. 4, pp. 330–338, 1993.

55. Kilmer, S. L., Lee, M. S., Grevelink, J. M., Flotte, T. J., and Anderson, R. R., "The Q-switched Nd: YAG laser effectively treats tattoos: a controlled, dose-response study," *Archives of Dermatology*, Vol. 129, no. 8, pp. 971–978, 1993.

56. Jones, A., Roddey, P., Orengo, I., and Rosen, T., "The Q-switched ND: YAG Laser Effectively Treats Tattoos in Darkly Pigmented Skin," *Dermatologic Surgery*, Vol. 22, no. 12, pp. 999–1001, 1996.

57. Goldberg, D. J., and Silapunt, S., "Histologic Evaluation of a Q-switched Nd: YAG Laser in the Nonablative Treatment of Wrinkles," *Dermatologic Surgery*, Vol. 27, no. 8, pp. 744–746, 2001.

58. Trelles, M. A., Alvarez, X., Martin-Vazquez, M. J., Trelles, O., Velez, M., Levy, J. L., and Allones, I., "Assessment of the efficacy of nonablative long-pulsed 1064-nm Nd: YAG laser treatment of wrinkles compared at 2, 4, and 6 months," *Facial Plastic Surgery*, Vol. 21, no. 2, pp. 145–153, 2005.

59. Hong, J. S., Park, S. Y., Seo, K. K., Goo, B. L., Hwang, E. J., Park, G. Y., and Eun, H. C., "Long pulsed 1064 nm Nd: YAG laser treatment for wrinkle reduction and skin laxity: evaluation of new parameters," *International Journal of Dermatology*.

60. White, J. M., Goodis, H. E., and Rose, C. L., "Use of the pulsed Nd: YAG laser for intraoral soft tissue surgery," *Lasers in Surgery and Medicine*, Vol. 11, no. 5, pp. 455–461, 1991.

61. Powell, J. L., Bailey, C. L., Coopland, A. T., Otis, C. N., Frank, J. L., and Meyer, I., "Nd: YAG laser excision of a giant gingival pyogenic granuloma of pregnancy," *Lasers in Surgery and Medicine*, Vol. 14, no. 2, pp. 178–183, 1994.

62. Bradley, P. F., "A review of the use of the neodymium YAG laser in oral and maxillofacial surgery," *British Journal of Oral and Maxillofacial Surgery*, Vol. 35, no. 1, pp. 26–35, 1997.

63. Costello, A. J., Bowsher, W. G., Bolton, D. M., Braslis, K. G., and Burt, J., "Laser Ablation of the Prostate in Patients with Benign Prostatic Hypertrophy," *British Journal of Urology*, Vol. 69, no. 6, pp. 603–608, 1992.

64. Costello, A. J., Johnson, D. E., and Bolton, D. M., “Nd: YAG laser ablation of the prostate as a treatment for benign prostatic hypertrophy,” *Lasers in Surgery and Medicine*, Vol. 12, no. 2, pp. 121–124, 1992.

65. Bozkulak, O., Tabakoglu, H. O., Aksoy, A., Kurtkaya, O., Sav, A., Canbeyli, R., and Gulsoy, M., “The 980-nm diode laser for brain surgery: histopathology and recovery period,” *Lasers in Medical science*, Vol. 19, no. 1, pp. 41–47, 2004.

66. Gulsoy, M., Dereli, Z., Tabakoglu, H. O., and Bozkulak, O., “Closure of skin incisions by 980-nm diode laser welding,” *Lasers in Medical science*, Vol. 21, no. 1, pp. 5–10, 2006.

67. Romanos, G., and Nentwig, G. H., “Diode laser (980 nm) in oral and maxillofacial surgical procedures: clinical observations based on clinical applications,” *Journal of Clinical Laser Medicine and Surgery*, Vol. 17, no. 5, pp. 193–197, 1999.

68. Wendt-Nordahl, G., Huckele, S., Honeck, P., Alken, P., Knoll, T., Michel, M. S., and Häcker, A., “980-nm diode laser: a novel laser technology for vaporization of the prostate,” *European Urology*, Vol. 52, no. 6, pp. 1723–1728, 2007.

69. Erol, A., Cam, K., Tekin, A., Memik, O., Coban, S., and Ozer, Y., “High power diode laser vaporization of the prostate: preliminary results for benign prostatic hyperplasia,” *The Journal of Urology*, Vol. 182, no. 3, pp. 1078–1082, 2009.

70. Yang, S. S., Hsieh, C. H., Lee, Y. S., and Chang, S. J., “Diode laser (980 nm) enucleation of the prostate: a promising alternative to transurethral resection of the prostate,” *Lasers in Medical science*, Vol. 28, no. 2, pp. 353–360, 2013.

71. Navarro, L., Min, R. J., and Boné, C., “Endovenous laser: a new minimally invasive method of treatment for varicose veins-preliminary observations using an 810 nm diode laser.,” *Dermatologic Surgery*, Vol. 27, no. 2, pp. 117–122, 2001.

72. Furtado de Medeiros, C. A., and Luccas, G. C., “Comparison of Endovenous Treatment with an 810 nm Laser versus Conventional Stripping of the Great Saphenous Vein in Patients with Primary Varicose Veins,” *Lasers in Medical science*, Vol. 31, no. 12, pp. 1685–1694, 2005.

73. Friberg, T. R., and Karatza, E. C., “The treatment of macular disease using a micropulsed and continuous wave 810-nm diode laser,” *Ophthalmology*, Vol. 104, no. 12, pp. 2030–2038, 1997.

74. Olk, R. J., Friberg, T. R., Stickney, K. L., Akduman, L., Wong, K. L., Chen, M. C., Levy, M. H., Garcia, C. A., and Morse, L. S., “Therapeutic benefits of infrared (810-nm) diode laser macular grid photocoagulation in prophylactic treatment of nonexudative age-related macular degeneration: two-year results of a randomized pilot study,” *Ophthalmology*, Vol. 106, no. 11, pp. 2082–2090, 1999.

75. *Eye-safe Lasers*, RP Photonics Encyclopedia. Available: http://www.rp-photonics.com/eye_safe_lasers.html.

76. Fried, N. M., “Thulium fiber laser lithotripsy: An in vitro analysis of stone fragmentation using a modulated 110-watt thulium fiber laser at 1.94 μm,” *Lasers in Surgery and Medicine*, Vol. 37, no. 1, pp. 53–58, 2005.

77. Scott, N. J., Cilip, C. M., and Fried, N. M., “Thulium fiber laser ablation of urinary stones through small-core optical fibers,” *Selected Topics in Quantum Electronics, IEEE Journal of*, Vol. 15, no. 2, pp. 435–440, 2009.

78. Blackmon, R. L., Irby, P. B., and Fried, N. M., "Holmium: YAG (λ = 2,120 nm) versus Thulium fiber (λ = 1,908 nm) laser lithotripsy," *Lasers in Surgery and Medicine*, Vol. 42, no. 3, pp. 232–236, 2010.

79. Ngo, A. K., Sharma, U., Kang, J. U., and Fried, N. M., "Laser welding of urinary tissues, ex vivo, using a tunable thulium fiber laser," in *Biomedical Optics 2006*, pp. 60781B–60781B, International Society for Optics and Photonics, 2006.

80. Blokker, R. S., Lock, T. M., and de Boorder, T., "Comparing Thulium Laser and Nd: YAG laser in the Treatment of Genital and Urethral Condylomata Acuminata in Male Patients," *Lasers in Surgery and Medicine*, Vol. 45, no. 9, pp. 582–588, 2013.

81. Xia, S. J., Zhang, Y. N., Lu, J., Sun, X. W., Zhang, J., Zhu, Y. Y., and Li, W. G., "Thulium laser resection of prostate-tangerine technique in treatment of benign prostate hyperplasia," *Zhonghua Yi Xue Za Zhi*, Vol. 85, no. 45, pp. 3225–3228, 2005.

82. Xia, S. J., Zhuo, J., Sun, X. W., Han, B. M., Shao, Y., and Zhang, Y. N., "Thulium laser versus standard transurethral resection of the prostate: a randomized prospective trial," *European Urology*, Vol. 53, no. 2, pp. 382–390, 2008.

83. Verdaasdonk, R., Rem, A. I., van Thoor, S., de Boorder, T., Klaessens, J., and Teichmann, H. O., "Comparison of the CO_2, cw Thulium and Diode laser in a thermal imaging model for the optimization of various clinical applications," in *Biomedical Optics 2006*, pp. 60840J–60840J, International Society for Optics and Photonics, 2006.

84. Fried, N. M., and Murray, K. E., "High-power thulium fiber laser ablation of urinary tissues at 1.94 μm," *Journal of Endourology*, Vol. 19, no. 1, pp. 25–31, 2005.

85. Theisen-Kunde, D., Tedsen, S., Herrmann, K., Danicke, V., and Brinkmann, R., "Partial kidney resection based on 1.94 μm fiber laser system," in *European Conference on Biomedical Optics*, p. 6632_4, Optical Society of America, 2007.

86. Keller, M. D., Stafford, J. A., Schmidt, B. P., and Wells, J. D., "In vitro testing of dual-mode thulium microsurgical laser," in *SPIE BiOS*, pp. 820711–820711, International Society for Optics and Photonics, 2012.

87. Tunc, B., and Gulsoy, M., "Tm: Fiber laser ablation with real-time temperature monitoring for minimizing collateral thermal damage: ex vivo dosimetry for ovine brain," *Lasers in Surgery and Medicine*, Vol. 45, no. 1, pp. 48–56, 2013.

88. Guney, M., Tunc, B., and Gulsoy, M., "Investigating the ablation efficiency of a 1940-nm thulium fibre laser for intraoral surgery," *International Journal of Oral and Maxillofacial Surgery*, Vol. 43, no. 8, pp. 1015–1021, 2014.

89. Tiburtius, C., Gross, A. J., and Netsch, C., "A prospective, randomized comparison of a 1940 nm and a 2013 nm thulium: yttrium-aluminum-garnet laser device for Thulium VapoEnucleation of the prostate (ThuVEP): First results," *Indian Journal of Urology*, Vol. 3, no. 1, p. 47, 2015.

90. Parsa, P., Jacques, S. L., and Nishioka, N. S., "Optical properties of rat liver between 350 and 2200 nm," *Applied optics*, Vol. 28, no. 12, pp. 2325–2330, 1989.

91. Ritz, J.-P., Roggan, A., Isbert, C., Müller, G., Buhr, H. J., and Germer, C.-T., "Optical properties of native and coagulated porcine liver tissue between 400 and 2400 nm," *Lasers in surgery and medicine*, Vol. 29, no. 3, pp. 205–212, 2001.

92. Germer, C. T., Roggan, A., Ritz, J. P., Isbert, C., Albrecht, D., Müller, G., and Buhr, H. J., "Optical properties of native and coagulated human liver tissue and liver metastases in the near infrared range," *Lasers in surgery and medicine*, Vol. 23, no. 4, pp. 194–203, 1998.

93. Matsumoto, R., Selig, A. M., Colucci, V. M., and Jolesz, F. A., "Interstitial Nd: YAG laser ablation in normal rabbit liver: Trial to maximize the size of laser-induced lesions," *Lasers in surgery and medicine*, Vol. 12, no. 6, pp. 650–658, 1992.

94. Sibille, A., Ponchon, T., Berger, F., and Lambert, R., "Pulsed versus continuous wave Nd-YAG laser-induced necrosis: Comparison in the rat liver in vivo," *Lasers in Medical Science*, Vol. 10, no. 1, pp. 47–53, 1995.

95. Orth, K., Russ, D., Duerr, J., Hibst, R., Steiner, R., and Beger, H. G., "Thermo-controlled device for inducing deep coagulation in the liver with the Nd: YAG laser," *Lasers in surgery and medicine*, Vol. 20, no. 2, pp. 149–156, 1997.

96. Ritz, J. P., Isbert, C. M., Roggan, A., Wacker, F., Buhr, H. J., and Germer, C. T., "Laser-induced thermotherapy: an in-situ ablation technique for the local treatment of irresectable colorectal liver metastases," in *EOS/SPIE European Biomedical Optics Week*, pp. 87–94, International Society for Optics and Photonics, 2000.

97. Ishikawa, T., Zeniya, M., Hokari, A., Kawabe, T., Suzuki, K., Fujise, K., and Toda, G., "An experimental study on Nd-YAG laser induced thermotherapy: Its possible application of the laser irradiation for therapy of hepatocellular carcinoma," *Hepatology Research*, Vol. 23, no. 1, pp. 25–30, 2002.

98. Ishikawa, T., Zeniya, M., Fujise, K., Hokari, A., and Toda, G., "Clinical application of Nd: YAG laser for the treatment of small hepatocellular carcinoma with new shaped laser probe," *Lasers in Surgery and Medicine*, Vol. 35, no. 2, pp. 135–139, 2004.

99. Jacques, S. L., Rastegar, S., Motamedi, M., Thomsen, S. L., Schwartz, J. A., Torres, J. H., and Mannonen, I., "Liver photocoagulation with diode laser (805 nm) versus Nd: YAG (1064 nm)," in *OE/LASE'92*, pp. 107–117, International Society for Optics and Photonics, 1992.

100. Wohlgemuth, W. A., Wamser, G., Reiss, T., Wagner, T., and Bohndorf, K., "In vivo laser-induced interstitial thermotherapy of pig liver with a temperature-controlled diode laser and MRI correlation," *Lasers in Surgery and Medicine*, Vol. 29, no. 4, pp. 374–378, 2001.

101. Rohde, E., Mesecke-von Rheinbaben, I., Roggan, A., Podbielska, H., Hopf, M., and Müller, G., "Interstitial laser-induced thermotherapy (LITT): comparison of in-vitro irradiation effects of Nd: YAG (1064 nm) and diode (940 nm) laser," *Medical Laser Application*, Vol. 16, no. 2, pp. 81–90, 2001.

102. Nikfarjam, M., Malcontenti-Wilson, C., and Christophi, C., "Comparison of 980-and 1064-nm wavelengths for interstitial laser thermotherapy of the liver," *Photomedicine and Laser Therapy*, Vol. 23, no. 3, pp. 284–288, 2005.

103. Nishioka, N. S., and Domankevitz, Y., "Comparison of tissue ablation with pulsed holmium and thulium lasers," *Quantum Electronics, IEEE Journal of*, Vol. 26, no. 12, pp. 2271–2275, 1990.

104. Theisen-Kunde, D., Wolken, H., Danicke, V., Brinkmann, R., Bruch, H., and Kleemann, M., "In vivo study of partial liver resection on pigs using a 1.9 μm thulium fiber laser," in *European Conferences on Biomedical Optics*, pp. 809211–809211, International Society for Optics and Photonics, 2011.

105. Merigo, E., Clini, F., Fornaini, C., Oppici, A., Paties, C., Zangrandi, A., Fontana, M., Rocca, J.-P., Meleti, M., Manfredi, M., *et al.*, "Laser-assisted surgery with different wavelengths: a preliminary ex vivo study on thermal increase and histological evaluation," *Lasers in Medical Science*, Vol. 28, no. 2, pp. 497–504, 2013.

106. Jansen, E. D., van Leeuwen, T. G., Motamedi, M., Borst, C., and Welch, A. J., "Temperature dependence of the absorption coefficient of water for midinfrared laser radiation," *Lasers in Surgery and Medicine*, Vol. 14, no. 3, pp. 258–268, 1994.

107. Lange, B. I., Brendel, T., and Hüttmann, G., "Temperature dependence of light absorption in water at holmium and thulium laser wavelengths," *Applied Optics*, Vol. 41, no. 27, pp. 5797–5803, 2002.

108. Walsh, J. T., and Cummings, J. P., "Effect of the dynamic optical properties of water on midinfrared laser ablation," *Lasers in Surgery and Medicine*, Vol. 15, no. 3, pp. 295–305, 1994.

109. "Recent Advances in Oral and Maxillofacial Surgery," in *Textbook of Oral and Maxillofacial Surgery* (Malik, N. A., ed.), ch. 17, p. 946, New Delhi: Jaypee Brothers Medical Publishers, 3 ed., 2012.

110. Youn, J. I., and Holcomb, J. D., "Ablation efficiency and relative thermal confinement measurements using wavelengths 1,064, 1,320, and 1,444 nm for laser-assisted lipolysis," *Lasers in Lasers in Medical Science*, Vol. 28, no. 2, pp. 519–527, 2013.

111. Perry, D. A., Goodis, H. E., and White, J. M., "In vitro study of the effects of Nd: YAG laser probe parameters on bovine oral soft tissue excision," *Lasers in Surgery and Medicine*, Vol. 20, no. 1, pp. 39–46, 1997.

112. Malskat, W. S. J., Stokbroekx, M. A. L., van der Geld, C. W. M., Nijsten, T. E. C., and van den Bos, R. R., "Temperature profiles of 980-and 1,470-nm endovenous laser ablation, endovenous radiofrequency ablation and endovenous steam ablation," *Lasers in Lasers in Medical Science*, Vol. 29, no. 2, pp. 423–429, 2014.

113. Van Nimwegen, S. A., L'Eplattenier, H. F., Rem, A. I., Van Der Lugt, J. J., and Kirpensteijn, J., "Nd: YAG surgical laser effects in canine prostate tissue: temperature and damage distribution," *Physics in Medicine and Biology*, Vol. 54, no. 1, p. 29, 2009.

114. Ishihara, M., Arai, T., Sato, S., Morimoto, Y., Obara, M., and Kikuchi, M., "Measurement of the surface temperature of the cornea during ArF excimer laser ablation by thermal radiometry with a 15-nanosecond time response," *Lasers in Surgery and Medicine*, Vol. 30, no. 1, pp. 54–59, 2002.

115. Cummings, J. P., and Walsh Jr, J. T., "Tissue tearing caused by pulsed laser-induced ablation pressure," *Applied Optics*, Vol. 32, no. 4, pp. 494–503, 1993.

116. *Brain Facts and Figures*. Available: https://faculty.washington.edu/chudler/facts.html.

117. Cheong, W. F., Prahl, S. A., and Welch, A. J., "A review of the optical properties of biological tissues," *IEEE Journal of Quantum Electronics*, Vol. 26, no. 12, pp. 2166–2185, 1990.

118. Sandell, J. L., and Zhu, T. C., "A review of in-vivo optical properties of human tissues and its impact on PDT," *Journal of Biophotonics*, Vol. 4, no. 11-12, pp. 773–787, 2011.

119. Vogel, A., and Venugopalan, V., "Mechanisms of pulsed laser ablation of biological tissues," *Chemical Reviews*, Vol. 103, no. 2, pp. 577–644, 2003.

120. van Hillegersberg, R., Pickering, J. W., Aalders, M., and Beek, J. F., “Optical properties of rat liver and tumor at 633 nm and 1064 nm: photofrin enhances scattering,” *Lasers in Surgery and Medicine*, Vol. 13, no. 1, pp. 31–39, 1993.